

Dany-Knedlik, Geraldine; Holtemöller, Oliver

Working Paper

Inflation dynamics during the financial crisis in Europe: Cross-sectional identification of long-run inflation expectations

IWH Discussion Papers, No. 10/2017

Provided in Cooperation with:

Halle Institute for Economic Research (IWH) – Member of the Leibniz Association

Suggested Citation: Dany-Knedlik, Geraldine; Holtemöller, Oliver (2017) : Inflation dynamics during the financial crisis in Europe: Cross-sectional identification of long-run inflation expectations, IWH Discussion Papers, No. 10/2017, Leibniz-Institut für Wirtschaftsforschung Halle (IWH), Halle (Saale), <https://nbn-resolving.de/urn:nbn:de:gbv:3:2-82318>

This Version is available at:

<https://hdl.handle.net/10419/172482>

Standard-Nutzungsbedingungen:

Die Dokumente auf EconStor dürfen zu eigenen wissenschaftlichen Zwecken und zum Privatgebrauch gespeichert und kopiert werden.

Sie dürfen die Dokumente nicht für öffentliche oder kommerzielle Zwecke vervielfältigen, öffentlich ausstellen, öffentlich zugänglich machen, vertreiben oder anderweitig nutzen.

Sofern die Verfasser die Dokumente unter Open-Content-Lizenzen (insbesondere CC-Lizenzen) zur Verfügung gestellt haben sollten, gelten abweichend von diesen Nutzungsbedingungen die in der dort genannten Lizenz gewährten Nutzungsrechte.

Terms of use:

Documents in EconStor may be saved and copied for your personal and scholarly purposes.

You are not to copy documents for public or commercial purposes, to exhibit the documents publicly, to make them publicly available on the internet, or to distribute or otherwise use the documents in public.

If the documents have been made available under an Open Content Licence (especially Creative Commons Licences), you may exercise further usage rights as specified in the indicated licence.



Halle Institute for Economic Research
Member of the Leibniz Association

Discussion Papers

No. 10

December 2017



Inflation Dynamics During the Financial Crisis in Europe: Cross-sectional Identification of Long-run Inflation Expectations

Geraldine Dany-Knedlik, Oliver Holtemöller

Authors

Geraldine Dany-Knedlik

Halle Institute for Economic Research (IWH) –
Member of the Leibniz Association,
Department of Macroeconomics, and
Martin-Luther University Halle-Wittenberg
E-mail: geraldine.dany@iwh-halle.de

Oliver Holtemöller

Halle Institute for Economic Research (IWH) –
Member of the Leibniz Association,
Department of Macroeconomics, and
Martin-Luther University Halle-Wittenberg
E-mail: oliver.holtemoeller@iwh-halle.de
Tel +49 345 7753 800

The responsibility for discussion papers lies solely with the individual authors. The views expressed herein do not necessarily represent those of IWH. The papers represent preliminary work and are circulated to encourage discussion with the authors. Citation of the discussion papers should account for their provisional character; a revised version may be available directly from the authors.

Comments and suggestions on the methods and results presented are welcome.

IWH Discussion Papers are indexed in RePEc-EconPapers and in ECONIS.

Editor

Halle Institute for Economic Research (IWH) –
Member of the Leibniz Association

Address: Kleine Maerkerstrasse 8
D-06108 Halle (Saale), Germany
Postal Address: P.O. Box 11 03 61
D-06017 Halle (Saale), Germany

Tel +49 345 7753 60
Fax +49 345 7753 820

www.iwh-halle.de

ISSN 2194-2188

Inflation Dynamics During the Financial Crisis in Europe: Cross-sectional Identification of Long-run Inflation Expectations

Abstract

We investigate drivers of Euro area inflation dynamics using a panel of regional Phillips curves and identify long-run inflation expectations by exploiting the cross-sectional dimension of the data. Our approach simultaneously allows for the inclusion of country-specific inflation and unemployment-gaps, as well as time-varying parameters. Our preferred panel specification outperforms various aggregate, uni- and multivariate unobserved component models in terms of forecast accuracy. We find that declining long-run trend inflation expectations and rising inflation persistence indicate an altered risk of inflation expectations de-anchoring. Lower trend inflation, and persistently negative unemployment-gaps, a slightly increasing Phillips curve slope and the downward pressure of low oil prices mainly explain the low inflation rate during the recent years.

Keywords: inflation dynamics, inflation expectations, trend inflation, nonlinear state space model, panel UCSV model, Euro area

JEL Classification: C32, E5, E31

1 Introduction

Headline inflation in the Euro area has been below the medium-term inflation target of the European Central Bank (ECB) for several years now. The year-on-year change in harmonized consumer prices has even been negative in early 2015 and again in early 2016. Understanding why inflation rates have been so low is important for assessing past and designing future monetary policy and for forecasting inflation. This has been stressed, among others, by central bankers, see for example the speech given by the vice president of the ECB at the Jackson Hole Economic Symposium in August 2015 (Constâncio, 2015).

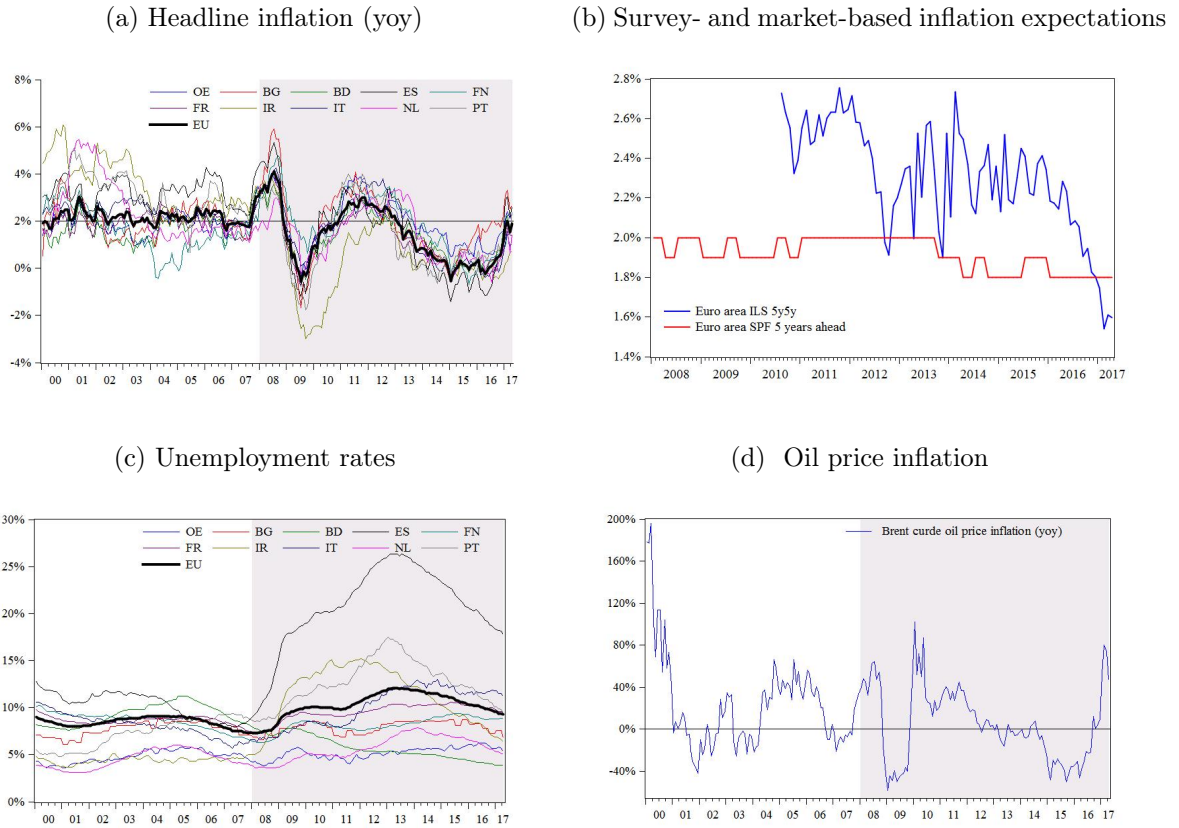
The New-Keynesian Phillips curve (NKPC) delivers a framework for the analysis of inflation dynamics. According to the NKPC, inflation is driven by expectations about future inflation, marginal costs of production and cost-push shocks including oil prices. Marginal costs which are difficult to measure are often approximated by an indicator of economic slack like output gap or the difference between actual unemployment and long-run average (or structural) unemployment (unemployment-gap). Figure 1 shows (a) headline inflation rates in the Euro area and in ten member countries of the European Monetary Union (EMU), (b) two indicators for inflation expectations, (c) unemployment rates, and (d) oil price changes. As the figure reveals, the possible inflation drivers may all have contributed to the low inflation rate in recent years. However, the coefficients in estimated Phillips curves may vary over time (Blanchard et al., 2015).

In the Euro area, estimating relations with time-varying parameters is difficult because the Euro has only been introduced in 1999 which implies relatively short time-series. Furthermore, there is evidence for the U.S. that regional Phillips curves are more stable than an aggregated national Phillips curve (Fitzgerald et al., 2013). In this paper, we propose a new methodology to estimate a panel of country-specific Phillips curves exploiting the cross-sectional dimension of inflation data in the Euro area. We specify and estimate a panel non-linear unobserved component stochastic volatility (UCSV) Phillips curve model (Cogley et al., 2010; Stella and Stock, 2013) using country-specific data for

Austria, Belgium, Germany, Ireland, Italy, Finland, France, the Netherlands, Portugal and Spain (hereafter we refer to this country group as EU10) and allowing for time-varying parameters. We show that this model has a very good forecasting performance compared to alternative specifications that have been proposed in the literature. From the estimated model we infer to what extent actual inflation in the Euro area has been driven by the various possible inflation drivers: long-run inflation expectations, unemployment-gaps and cost-push shocks. It turns out that economic slack in the Euro area as indicated by unemployment-gaps and decreasing oil prices can explain a large share of the inflation dynamics. However, there is also evidence that long-run inflation expectations have fallen below the ECB's medium-term inflation target, and that inflation persistence has increased in the Euro area. Since unemployment-gaps are currently closing in the Euro area due to the economic upswing and oil prices have been increasing recently our model predicts that headline inflation will also approach its long-run average value again. But because inflation persistence is higher than it used to be before the financial crisis convergence to the long-run average takes longer than before. Additionally, long-run inflation expectations have contributed about 0.5 percentage points to the decline in headline inflation and are still below the medium-term target according to our estimations. Therefore, inflation may be lower than the inflation target for a prolonged period. Long-run inflation expectations below the inflation target may be an indication of inflation de-anchoring which would be a major challenge for monetary policy (Blinder, 2000).

Overall, this paper adds to three strands of the literature, namely the literature on the modelling of inflation dynamics using non-linear UCSV specifications, the literature on long-run inflation expectations and inflation expectations (de-)anchoring in the Euro area, and the literature on changes in the inflation dynamics during and after the Great Recession. The paper is organized into eight sections. The second section provides a brief literature review and explains our contribution to the literature in more detail. The third section is dedicated to the empirical methodology, including the econometric model, data, and estimation details. In the fourth section, we present the empirical results of our benchmark model, including the contributions of the distinct factors to headline inflation

Figure 1: Euro area inflation dynamics and possible drivers



Source: We obtained the series of survey- and market-based inflation expectations from Consensus Economics, Thomson Reuters and our own calculations. For the remaining data sources we refer to the data and estimation section.

rates. The fifth section contains a comparison of our benchmark model to commonly used non-linear UCSV-models. In the sixth section, we undertake a forecasting exercise, comparing the forecast performance of our proposed panel structure to that of a variety of other inflation models. The seventh section includes a robustness analysis, and is followed by the last section, in which we offer a brief conclusion.

2 Literature Review

Unobserved component models for inflation dynamics have been used in the literature to decompose actual inflation into a long-run component - called ‘trend inflation’ - and short-run fluctuations. Chan et al. (2016) for example, estimate a non-linear Phillips curve for the U.S. and identify both trend inflation and the non-accelerating inflation rate

of unemployment (NAIRU). They show that their non-linear specification outperforms various vector autoregressive models as well as linear or partially non-linear unobserved components models in terms of forecasting accuracy. Garnier et al. (2015) propose a multivariate Beveridge-Nelson decomposition using various measures of inflation as well as measures of real economic activity to identify overall trend inflation and show that a multivariate trend specification improves forecast accuracy over univariate models. We combine the unobserved components approach with exploiting multivariate data by extending the non-linear unobserved component stochastic volatility (UCSV) model to panel data. At least to our knowledge, we are the first to estimate a Euro area Phillips curve identifying unobserved unemployment-gaps and allowing for time-varying coefficients.

Our estimated panel UCSV model implies model-compatible long-run inflation expectations. These can be compared to other measures of inflation expectations which have been constructed using survey data or derived from financial market prices. In several countries, survey-based inflation expectations measures have persistently predicted inflation rates above or below the actual inflation rates for extended periods. This raises the question whether these survey-based indicators are reliable measures for long-run inflation expectations, or whether they are systematically biased. Fuhrer et al. (2012) find that Japanese survey-based inflation expectations measures are persistently above actual inflation rates. Chan et al. (2017) find systematic time-varying deviations of survey-based expectations measures from trend inflation for the U.S., UK and Japan. It has been shown that social and psychological factors might drive the outcomes of survey-based inflation expectations.¹ Market-based inflation expectations can be extracted from break-even-inflation (EBI hereafter) rates based on inflation-indexed government bonds. However, EBI are only available for a few countries in the Euro area and are traded at low volumes, which complicates the estimation of possibly time-varying risk premiums. Therefore, empirical evidence on the accuracy of inflation expectations anchoring based

¹ Van der Klaauw et al. (2008) show that the phrasing of questions in the inflations-expectations survey of Reuters/University of Michigan Survey of Consumers led to distinct interpretations and increased dispersions in the answers given. Moreover, participants may provide what they deem to be a socially desirable answer in favour of the issuer of the questionnaire (Paulhus, 2002).

on EBI estimates is mixed.² Moreover, considering break-even inflation rates might not be a sensible way to estimate long-run inflation expectations due to their high volatility (Faust and Wright, 2013).

We also contribute to the literature on inflation dynamics during and after the Great Recession and the literature on the missing (dis-)inflation puzzle. For the U.S. case of missing disinflation Watson (2014) compared inflation predictions from traditional Phillips curve estimations with actual inflation during the global financial crisis and finds that inflation did not fall as predicted given the size of the unemployment-gap. He suggests that several factors could be at work including anchored inflation expectations, changes in inflation indexation and changes in the slope of the Phillips curve. Applying the non-linear Phillips curve specification of Matheson and Stavrev (2013) to 23 advanced economies, Blanchard et al. (2015) find that the slope of the Phillips curve significantly declined in the 1990s but has remained stable since then. Mertens (2016) shows that U.S. trend inflation declined in the course of the global financial crises and that at the same time uncertainty about the trend level increased. As in the U.S., the Euro area experienced inflation rates persistently above the predicted rates between 2008 to 2011. However, in the recovery phase of the sovereign debt crisis, the puzzle reversed, and headline inflation has been continuously over-predicted. Using a largescale vector autoregression Bobeica and Jarocinski (2017) show that the headline inflation dynamics in the Euro area can be mainly explained by global factors during the global financial crisis and by domestic factors from 2011 to 2014. Other empirical work by Riggi and Venditti (2015) and Jarociński and Lenza (2016) derives an alternative measure of output gap estimates that match inflation dynamics after the sovereign debt crisis. In contrast to large-scale empirical approaches, our panel UCSV model allows a structural interpretation of events, because our specification is based on a theoretically founded New-Keynesian Phillips Curve relationship.

²Nautz et al. (2017) apply a multiple break-point test to break-even inflation and found that the inflation expectations in the Euro area were well anchored until late 2011 but have since then significantly reacted to macroeconomic news. By contrast, Autrup and Grothe (2014) did not find any evidence of expectations de-anchoring in the Euro area following a similar approach like Nautz et al. (2017) but using a smaller time-span and different indicators to control for the liquidity risk premium.

3 Empirical Methodology

3.1 Baseline model

We estimate a non-linear, bivariate unobserved component model of the unemployment-based Phillips curve, similar to the models used by Chan et al. (2016) and Stella and Stock (2013). What differentiates our model from the aforementioned ones is that we introduce cross-sectional information for the identification of the long-run trend inflation and common time-varying parameters. Our benchmark model takes on the following form:

$$\begin{aligned}
 \pi_{n,t} - \tau_t^{\pi,EU} &= \rho_t^\pi (\pi_{n,t-1} - \tau_{t-1}^{\pi,EU}) + \lambda_t (u_{n,t} - \tau_{n,t}^u) + \beta_t \pi_t^{oil} + \epsilon_{n,t}^\pi \\
 u_{n,t} - \tau_{n,t}^u &= \rho_{n,1}^u (u_{n,t-1} - \tau_{n,t-1}^u) + \rho_{n,2}^u (u_{n,t-2} - \tau_{n,t-2}^u) + \epsilon_{n,t}^u \\
 \tau_t^{\pi,EU} &= \tau_{t-1}^{\pi,EU} + \epsilon_t^{\tau,\pi} \\
 \tau_{n,t}^u &= \tau_{n,t-1}^u + \epsilon_{n,t}^{\tau,u} \\
 \rho_t^\pi &= \rho_{t-1}^\pi + \epsilon_t^{\rho,\pi} \\
 \lambda_t &= \lambda_{t-1} + \epsilon_t^\lambda \\
 \beta_t &= \beta_{t-1} + \epsilon_t^\beta
 \end{aligned} \tag{1}$$

with $n = 1, \dots, N$ number of countries, $t = 1, \dots, T$ points in time. The first line reflects the Phillips curve relation, written in the inflation-gap formulation - that is the difference between $\pi_{n,t}$, the annualized quarter-on-quarter change of harmonized consumer prices (HICP), and $\tau_t^{\pi,EU}$, the unobserved trend inflation. In this Phillips curve specification, we assume that the current inflation-gap is explained by the past inflation-gap, the unemployment-gap and by a cost push factor, namely oil price inflation. The second row specifies the unemployment-gap - that is the deviation of unemployment rates from the non-accelerating inflation rate of unemployment (NAIRU) modelled as an AR(2) process. We allow all coefficients in the Phillips curve relation to be time-varying. We chose to do so because Stella and Stock (2013) have shown that allowing the persistence parameter to vary over time is empirically important. Additionally, we allow the level of the error variance to change over time and introduce a common stochastic volatility component in the inflation-gap equation. The error terms of the model can be summarised in the following way:

$$\begin{aligned}
\epsilon_{n,t}^\pi &\sim N(0, e^{h_t}) \\
h_t &= h_{t-1} + \epsilon_t^h \\
\epsilon_t^h &\sim N(0, \sigma_h^2) \\
\epsilon_{n,t}^u &\sim N(0, \sigma_{n,u}^2) \\
\epsilon^{\rho^\pi} &\sim TN(-\rho_{t-1}^\pi, 1 - \rho_{t-1}^\pi; 0, \sigma_{\rho^\pi}^2) \\
\epsilon^\lambda &\sim TN(-1 - \lambda_{t-1}, 0 - \lambda_{t-1}; 0, \sigma_\lambda^2) \\
\epsilon^\beta &\sim TN(-\beta_{t-1}, 1 - \beta_{t-1}; 0, \sigma_\beta^2)
\end{aligned} \tag{2}$$

As the literature on time-varying coefficients suggests, we assume that the Phillips curve parameters and the stochastic volatility evolve as driftless random walks (see among others Cogley et al. (2010), Stock and Watson (2007) or Chan et al. (2013)). As Chan et al. (2016) points out, the state specification of driftless random walks introduces excess uncertainty about the location of states when economic analysis of past developments allows a reasonable parameter space to be defined ex ante. Therefore, we introduce truncated distributions for λ , ρ_π and ρ_u . In particular, we assume that the slope, persistence and cost-push shock parameters lie within the intervals $(-1, 0)$, $(0, 1)$ and $(0, 1)$, respectively. The unemployment-gaps evolve as stationary AR(2) processes, implying that $\rho_{n,1}^u + \rho_{n,2}^u < 1$, $\rho_{n,2}^u - \rho_{n,1}^u < 1$ and $|\rho_{n,2}^u| < 1$. Due to interrelations between the latent variables $\tau_t^{\pi,EU}$, $\tau_{n,t}^u$, λ_t , ρ_t^π , β_t and h_t the model shown in equation (1) is non-linear.

3.2 Trend inflation, inflation expectations, and monetary policy

An important feature of our model specification is the decomposition of trend inflation and country-specific cyclical movements of inflation rates. This is so because changes in the trend and country-specific cyclical inflation components have different policy implications. Thus movements in trend inflation relate to changes in the long-run inflation and the degree of central bank credibility. By contrast, movements in country-specific inflation-gaps are driven by business cycle conditions, including the country's monetary policy stance and exogenous cost-push shocks. While there may be different long-run inflation trends in the countries of the Euro area, the ECB's monetary policy is only directed towards stabilizing Euro area average inflation. The Euro area average time-varying

inflation trend $\tau_t^{\pi,EU}$ is therefore important for monetary policy purposes. Model (1) implies that, in the long-run (in the absence of unemployment and oil price shocks) Euro area average inflation converges to $\tau_t^{\pi,EU}$. Therefore, period t 's model-based long-run inflation expectation for the Euro area as a whole is equal to $\tau_t^{\pi,EU}$. However, it could be that different countries in the Euro area follow different inflation trends. This is not captured by our model since country-specific unemployment-gaps $\pi_{n,t} - \tau_t^{\pi,EU}$ have a zero unconditional mean. Recall that our main purpose is not to estimate country specific inflation dynamics but to use country-specific information to identify Euro-area average dynamics, and model (1) is intended to be useful for understanding the overall Euro area inflation trend.

3.3 Data and Estimation

We use seasonally adjusted data on a monthly frequency for EU10 countries (Austria, Belgium, Finland, France, Germany, Ireland, Italy, the Netherlands, Portugal and Spain) from 1999m01 until 2017m04. As a measure for inflation we use the overall change in harmonized index of consumer prices (HICP hereafter) and corresponding country weights provided by the ECB Data Warehouse and Eurostat. The unemployment rate and underlying number of unemployed persons and labour force data are taken from Eurostat. We use the latter two data sets to calculate country-specific weights to construct hypothetical EU10 unemployment series. For oil prices, we use the Brent crude oil spot price from the U.S. Energy Information Administration (EIA). We calculate annualized quarter-on-quarter percentage changes for all series except the unemployment rate. Moreover, we de-mean the oil price inflation series.

We employ Bayesian estimation techniques to estimate latent states, parameters and variances. In particular, we use the precision-based MCMC algorithm proposed by Chan and Strachan (2012). Thus we rewrite our benchmark model, as in Chan et al. (2016), but include a panel dimension, in which we use the usual matrix notation of time-fixed effects in panel models (see for example Greene (2014)) to specify the common latent

states. The full derivation of conditional densities as well as the choice of prior and a prior sensitivity analysis are outlined in the technical appendix.

4 Results

We discuss our results in three steps. We begin by examining and interpreting the empirical results of our benchmark model in detail, including the inflation trend estimate, country-specific inflation-gaps, the country-specific NAIRUs and unemployment-gaps, as well as the estimates of time-varying parameters. Then we compare the key results of our benchmark model to the corresponding outcomes of various other inflation models that have recently been presented in the literature. Finally, we carry out a forecasting exercise, evaluating the forecasting performance of the panel-structured Phillips curve against that of a number of uni- and multivariate inflation models.

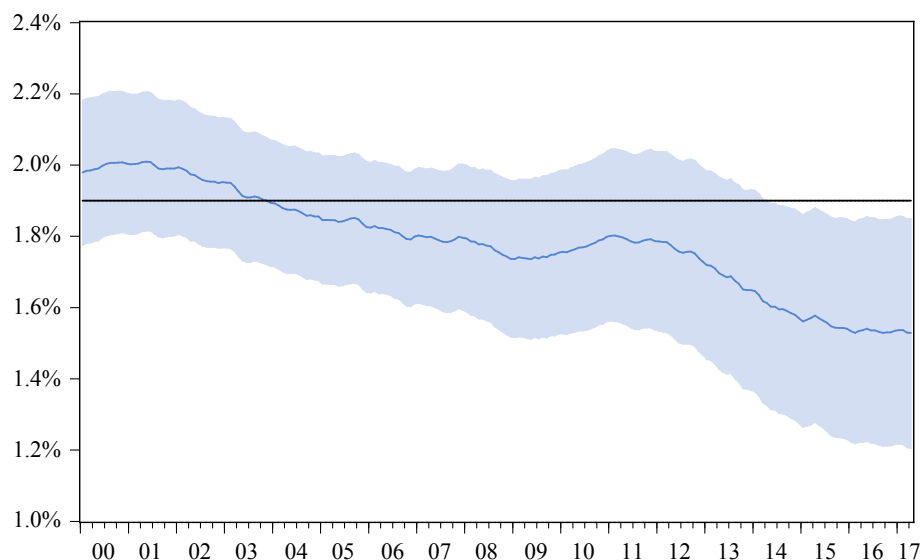
4.1 Empirical results of the baseline model

Trend inflation

The estimates of the trend inflation and the country-specific inflation-gaps are shown in Figures 2 as well as 3 and are discussed in turn, starting with trend inflation.

The estimates of the trend inflation are not significantly different from 1.9% between 1999 and 2013. This is in line with the ECB's inflation target of below (but close to) 2%. The posterior mean of trend inflation declined from 2% in 1999, and stabilized to 1.8% in the course of the global financial crisis. In mid-2013, the trough of the sovereign debt crisis (see CEPR Euro Area Business Cycle Dating), trend inflation started to fall significantly below 1.9%, and continued to decline to 1.5% in mid-2016. It stabilized thereafter. The upper and lower probability bands have the same quantitative magnitude of the survey-based and market-based inflation expectation measures in the last few years, amounting to 1.8% and 1.2%, respectively.

Figure 2: Trend inflation estimates



The solid line show the posterior means and the shaded area indicate the 95% probability bands

From a Phillips curve perspective, the anchoring of long-run inflation expectations is determined by two conditions. Firstly, long-run inflation expectations should equal the central bank's desired level of long-run inflation. Secondly, the inflation process should be predominantly driven by these long-run expectations (along with economic activity and cost-push shocks) rather than past inflation values. A deviation of either of these conditions is sufficient to cause a situation of de-anchored long-run inflation expectations. The former condition is approximated by our results on the trend inflation estimates in Figure 2. They reflect a continuous and significant deviation of long-run inflation expectations from the ECB's desired long-run inflation level from 2013 onwards. The latter condition relates to the persistence parameter and is discussed later in this section. Generally, our estimates indicate that persistently low headline inflation between 2013 to 2017 is at least partly driven by a decline in trend inflation and is not purely a cyclical and/or cost-push shock phenomenon.

Country-specific inflation-gaps

The dynamics of inflation-gap estimates shown in Figure 3 differed substantially across countries before the start of the global financial crisis, but appear to be homogeneous

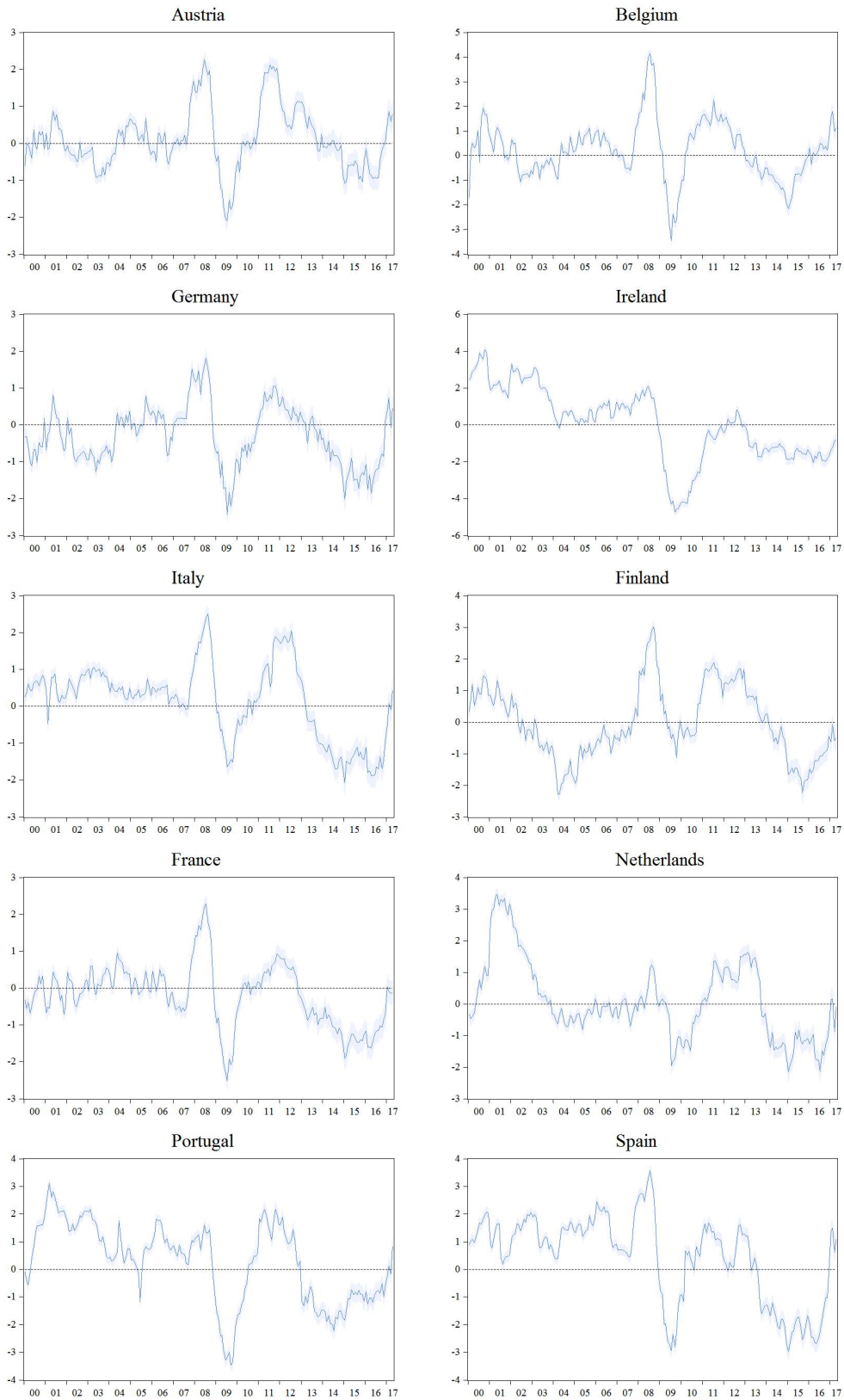
thereafter. In the pre-crisis period, Ireland, Italy, Portugal and Spain experienced persistently positive inflation-gaps - the average inflation-gap estimates for the pre-crisis period ranged from 0.64 for Italy to 1.63 for Portugal. By contrast, for Austria, Belgium, Germany, Finland and France, the inflation-gap estimates fluctuated evenly, with no persistent deviation in either direction. This heterogeneity of the inflation-gap estimates across countries, and especially the persistently positive inflation-gap estimates of the periphery countries in the pre-crisis episode, are consistent with empirical findings on causes of macroeconomic imbalances in the EMU. The literature suggests that inflation differentials can be related to an increase of unit labour costs and a rise of current account imbalances in periphery countries, due to the misallocation of capital across the EMU that led to persistent real exchange rate misalignments, rather than a catching-up effect in the tradeable sector (see Coudert et al. (2013) and references therein).

In the post-crisis period, the dynamics of inflation-gap estimates appeared much more homogeneous in quality and quantity across countries. Apart from substantial spikes in both directions around 2008 and 2009, inflation-gaps were persistently positive between 2010 to 2013, and peaked in 2012, at roughly 2% for most countries (except for Germany and France, where it was roughly 1%, and Ireland, where it was roughly 0.5%). Thereafter, the inflation-gaps turned negative and declined continuously until the end of 2016, with inflation-gaps around -2% for all countries, except for Austria (around -1%) and Spain (around -3%). Towards the end of the sample, inflation-gaps started to close again. Overall, the estimates suggest that headline inflation dynamics across EU10 countries were subject to amplified but relatively more homogeneous cyclical movements in the post-crisis period. Moreover, the sharp drop in the inflation-gaps between late 2012 to 2016 indicate that cyclical factors played an important role in explaining the period of low inflation in EU10 countries.

NAIRU and unemployment-gap estimates

Figure 4 illustrates the posterior means and 95% probability bands of the country-specific NAIRUs (blue lines and shading) together with the corresponding actual unemployment

Figure 3: Inflation-gap for EU10 countries in percentage points



Solid lines show the posterior means and shaded areas indicate the 95% probability bands

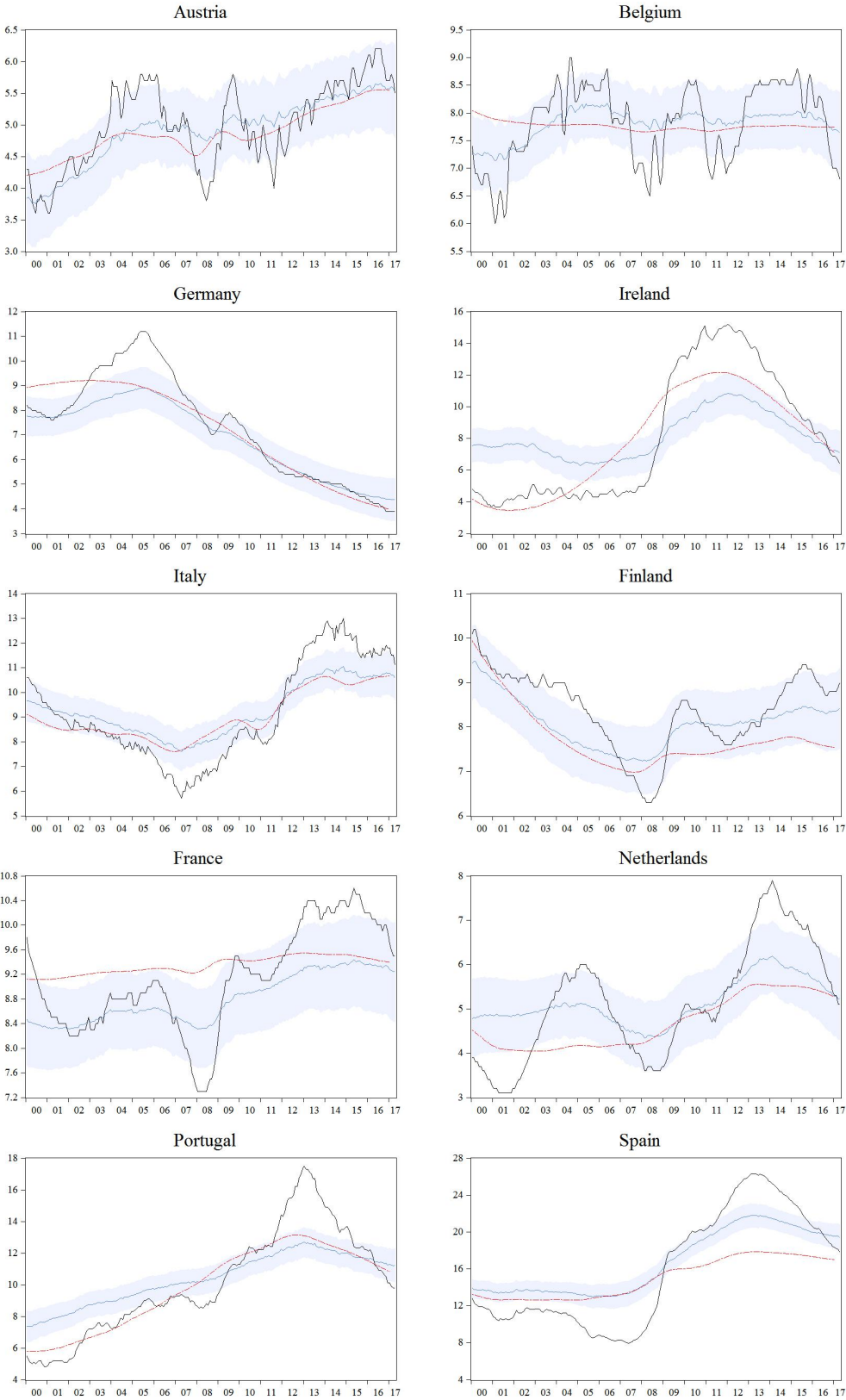
rates (black line), the NAWRU estimates of the European Commission (red line). Figure 5 shows the posterior means and 95% probability bands of the unemployment-gaps for each country. A striking feature of the actual, cyclical and structural unemployment rates across the EU10 countries is the continuous heterogeneity in both the levels and the dynamics.

For Ireland, Portugal, Spain and Italy, the NAIRU estimates increased significantly from the start of the financial crisis until the peak of the sovereign debt crisis, and declined thereafter. unemployment-gap estimates (see Figure 5) for this country group were primarily negative for the first part of the sample and turned positive in the course of the double dip recession, peaking at the height of the sovereign debt crisis and partly declining thereafter. Thus, prior to the crisis, these countries experienced reduced unemployment rates, mainly as a cyclical phenomenon, and structural unemployment was relatively stable. In the course of the double dip recession, however, the substantial increase in the unemployment rates for Ireland, Portugal, Spain and Italy originated from cyclical effects, as shown by positive unemployment-gaps of up to 5.7% (Spain), and from significant increases in structural unemployment rates. For example, Portugal's NAIRU increased by 4.2 percentage points from the beginning of global financial crisis up to the end of 2012.

By contrast, the NAIRU estimates of Austria, Belgium, France, Finland and the Netherlands (Figure 4) did not change significantly throughout the sample period. Germany was an exception, because the German NAIRU estimates declined continuously from 2005 onwards. These countries displayed positive unemployment-gaps around 2005 (except for France) and in the course of the recession (to lesser extent for Germany). While this group of countries experienced cyclical effects over the sample, estimates indicated no significant positive long-run effect on structural unemployment.

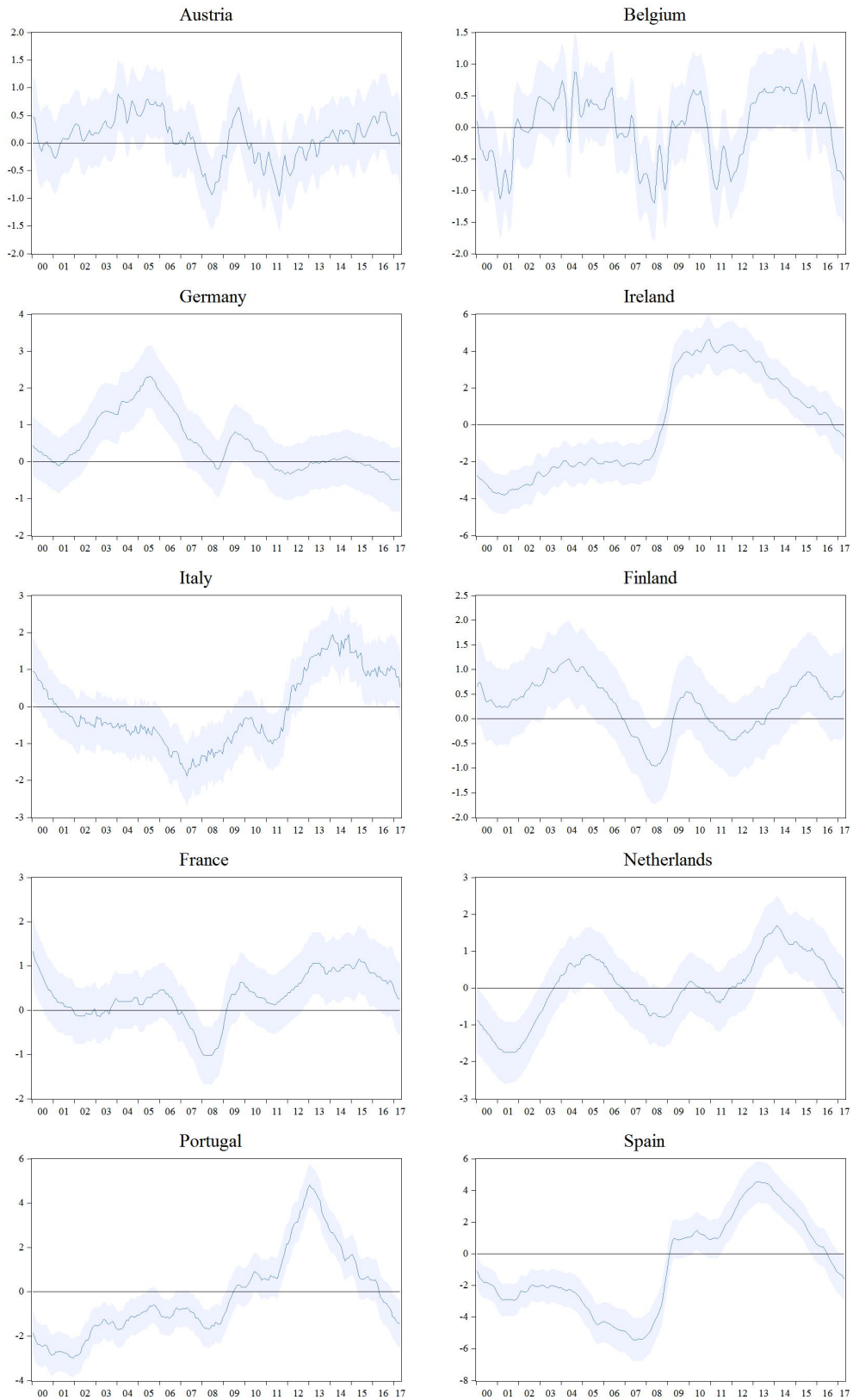
The asymmetries of the NAIRU and unemployment-gap estimates mirror the structural differences in the labour markets well, and reflect the severity of the financial and sovereign debt crisis across countries. Turning to the latter, Anderton et al. (2012) shows that

Figure 4: Estimated NAIRU and actual rate of unemployment for EU10 countries in percent



The solid blue lines show the posterior means, the blue shaded area indicate the 95% probability bands of NAIRU estimates, the red line indicates the NAWRU estimates of the EC and the black line depicts actual unemployment

Figure 5: Estimated unemployment-gap for EU10 countries in percentage points



The solid lines show the posterior means and the shaded areas indicate the 95% probability bands

elasticity estimates of GDP components to unemployment are substantially higher for domestic production than for exports. Discontinuity in the construction sector and/or accumulated competitiveness losses in Spain, Portugal, Ireland and Italy might partially explain the quantitatively higher increases of the unemployment-gaps from the beginning of the crisis in these countries, compared to the unemployment-gaps in the remaining countries. For Austria, Belgium, Germany, France, Finland and the Netherlands, where declines in exports were the main driver of the decrease in real economic activity, the effects of the Great Recession on the cyclical and structural unemployment dynamics are more limited.

The heterogeneous dynamics of our NAIRU estimates are also consistent with empirical findings on labour market performance, as well as differences in labour market institutions and structures across EU10 countries. Arpaia et al. (2014) report that countries that experienced a sector-specific boom prior to the crisis (such as the construction sector boom in Spain, Portugal and Ireland) faced a substantial increase in the degree of mismatch between the skills demanded by employees and those supplied by the unemployed on the labour market. The rise in the level of mismatch is to some extent permanent and therefore contributes to a rise in structural unemployment, because the existing human capital available from employees in those sectors that were hardly hit by the crisis might be of limited use for new jobs in expanding sectors.³

Another important determinant of structural unemployment dynamics is labour market and social benefit reforms. The most pronounced example is the labour market reform package that Germany introduced in the early 2000s. Consistent with the decline in our NAIRU estimates for Germany, Dustmann et al. (2014) found that the major reshaping of German labour market institutions, unemployment benefits and regulation lowered structural unemployment substantially and facilitated better labour market performance in the course of the crisis. The declining tendencies in the NAIRU estimates for Ireland, Italy, Portugal and Spain between 2013 and 2017 may be a result of ongoing labour market

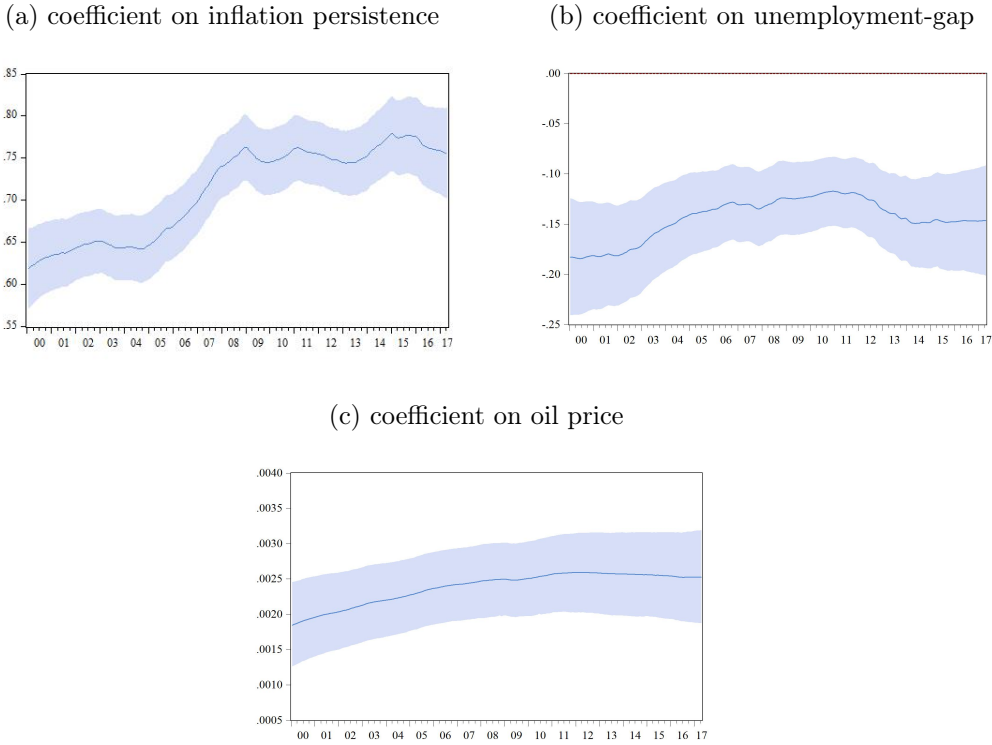
³This effect has been called 'hysteresis' as described in Ball (2009). The scope of our paper does not allow us to engage in the recent debate around hysteresis effects on unemployment.

reforms, as part of structural policy packages supporting the recovery from the sovereign debt crisis. Overall, our NAIRU estimates are well able to capture recent economic episodes and developments on labour markets for each country, respectively, and they also compare well to the NAWRU estimates of the European Commission. Given our model specification, the altered unemployment-gaps of the periphery countries should partially translate into declining EU10 headline inflation rates.

Time-varying Phillips curve parameters

Posterior means and 95% probability bands of the persistence coefficient, the Phillips curve slope and oil price coefficient are shown in Figure 6. Panel a of Figure 6 indicates that during the global financial crisis, inflation persistence increased significantly from around 0.65 between 1999 and 2006 to 0.75 from 2008 onwards. This implies that the degree of backward-lookingness of price setters has increased. This may relate to the credibility of the monetary policy regime (Erceg and Levin, 2003).

Figure 6: Time varying parameter estimates



The solid lines show the posterior means and the shaded areas indicate the 95% probability bands

In this sense the magnitude of inflation persistence reflects the agent's uncertainty about whether the central bank can accomplish its long-run inflation target. From a monetary policy perspective, this implies that in addition to a decline in the trend inflation below the desired long-run level of 1.9% (see the above discussion of trend inflation estimates), headline inflation has become less anchored to its long-run trend, indicating a rise in uncertainty from 2013 onwards about whether the ECB will be able to achieve its long-run inflation target.

The posterior mean of λ indicates that the Phillips curve for the EU10 countries is generally rather flat, averaging to -0.15 for the entire sample. Thereby, the posterior mean of the slope parameter reveals that the Phillips curve flattened throughout the period from early to mid-2000. The implied flattening of the EU10 Phillips curve is in line with the empirical evidence reported by Blanchard et al. (2015). In late 2013, however, the slope starts to increase again. Although the decline of λ is not significant, this could potentially explain missing inflation in the euro area. Riggi and Venditti (2015) also report that the elasticity of inflation with respect to real economic activity intensified in 2013 and 2014. The posterior mean of the oil price coefficient (Panel c, Figure 6) gradually increased from 0.0017 to 0.0023.

Decomposition of actual inflation

To show how different cyclical and long-run drivers affect headline inflation rates, we present the contribution of each of these factors to headline inflation rates across EU10 countries. We base the simulation of contributions on the posterior means of states and parameters. We also construct a hypothetical EU10 headline inflation rate, together with the consolidated contributions of the aforementioned inflation components. We do so by applying the official HICP weights provided by Eurostat to the country-specific headline inflation rates and corresponding contributions.

Figure 7: Contributions to inflation I/III

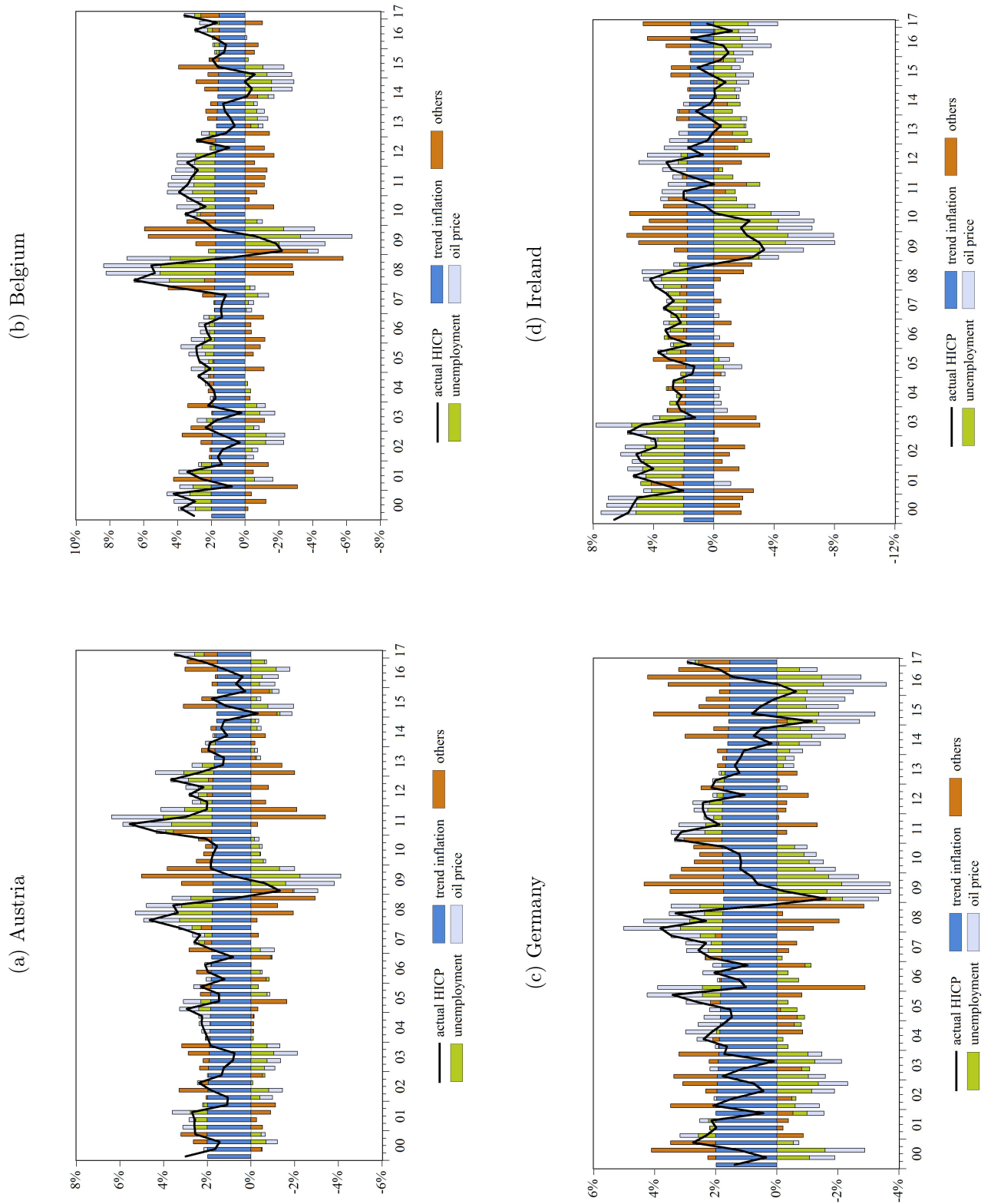


Figure 8: Contributions to inflation II/III

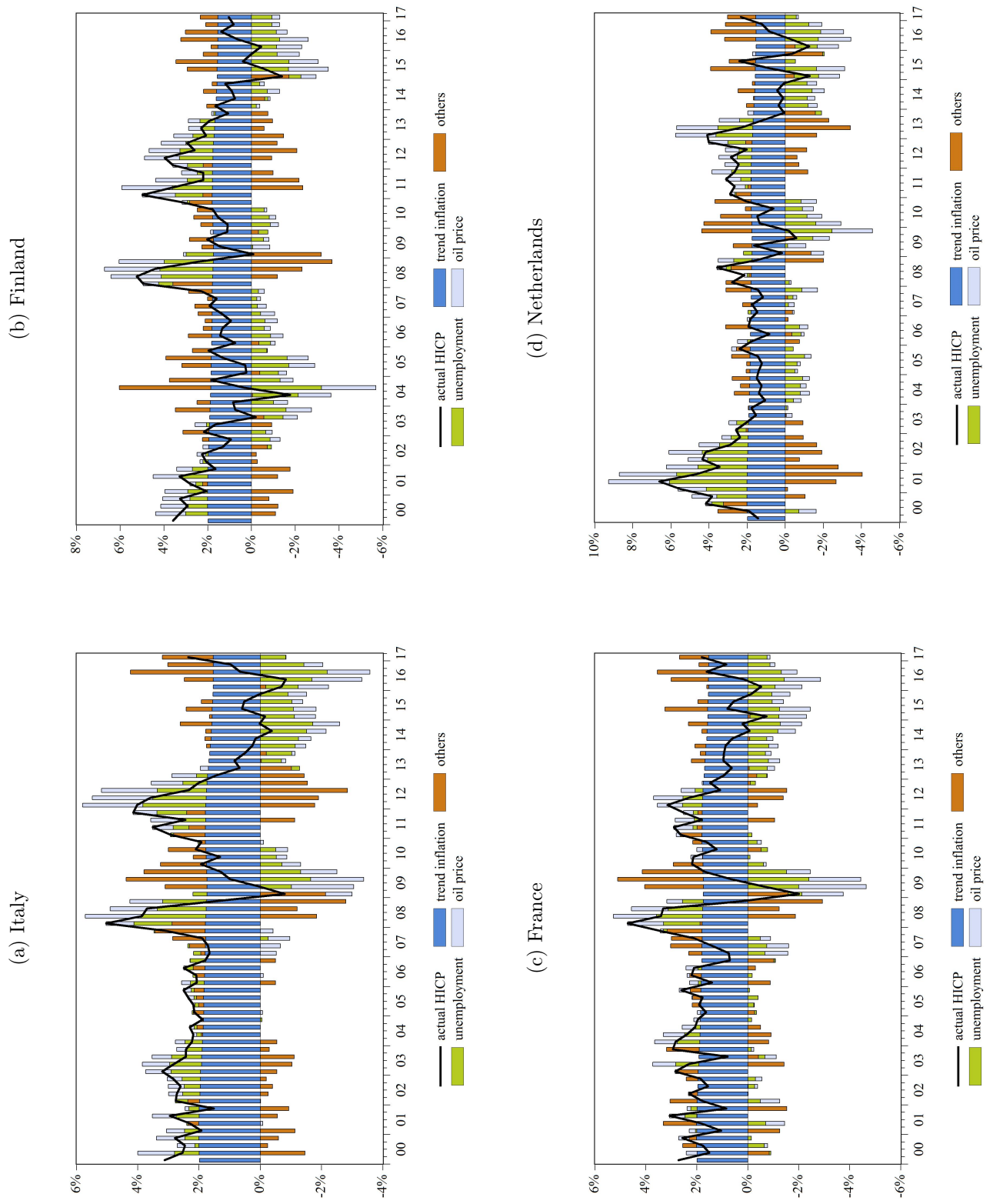
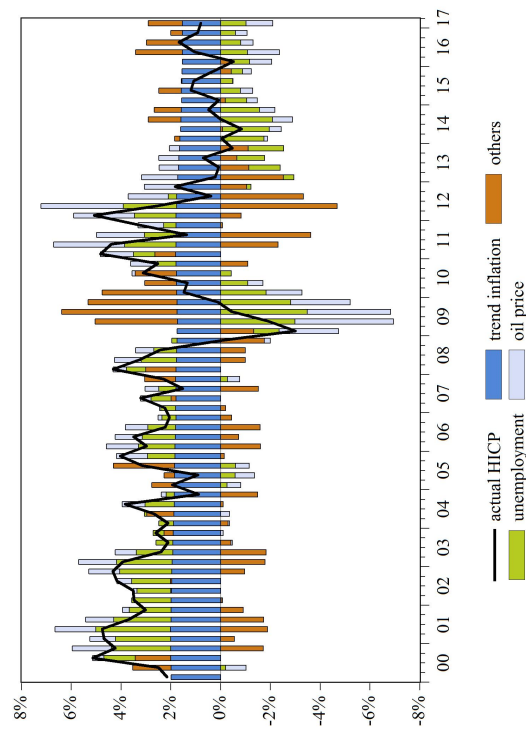


Figure 9: Contributions to inflation III/III

(a) Portugal



(b) Spain

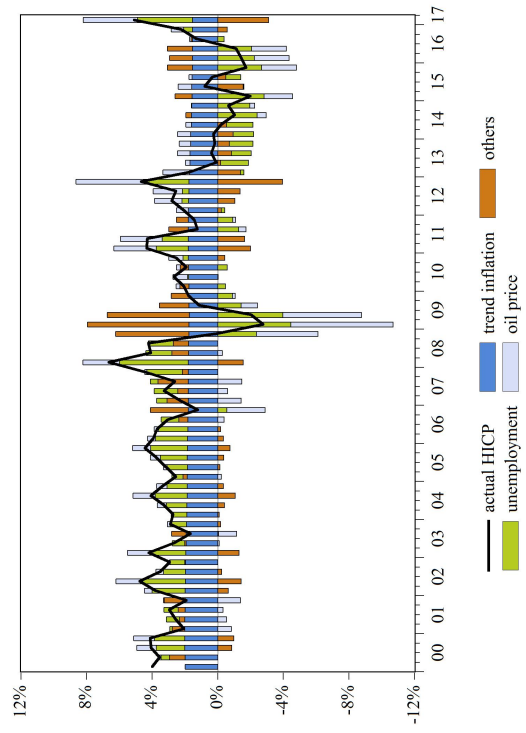
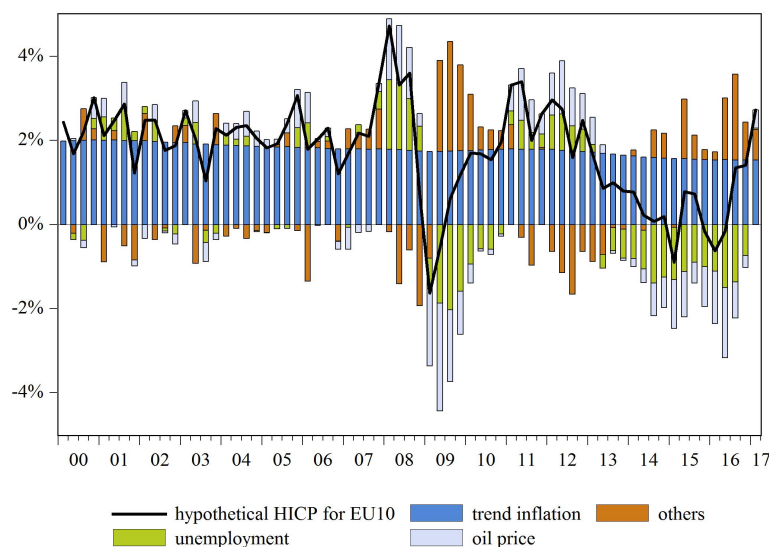


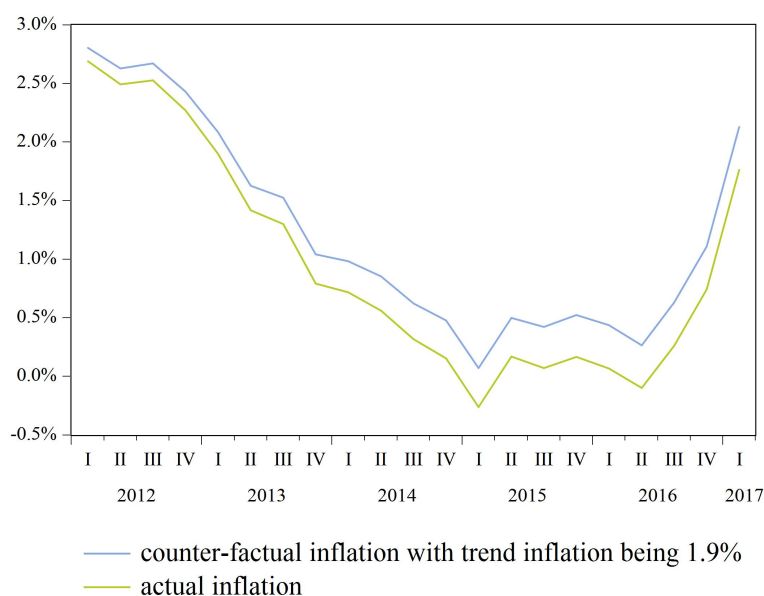
Figure 10: Hypothetical EU10 contributions



Across countries (see Figures 7, 8 and 9) the contribution of trend inflation explains quantitatively the largest share of headline inflation rates. Country-specific contributions assemble the dynamics of inflation and unemployment-gaps discussed in the previous section. We found that the dynamics of the contribution of unemployment and oil price inflation across countries were heterogeneous before the global financial crisis, but became more homogeneous from 2008 onwards. Thus the persistently higher headline inflation rates of periphery countries in the first half of the sample are partly a result of unemployment rates below the respective long-run unemployment trends. For example, the average contributions of unemployment from 1999M03 to 2007M12 amounted to 1.4% for Ireland, 0.4% for Italy, 1% for Portugal and 1.2% for Spain.

Low levels of German and Finish headline inflation in the early 2000s can, to some extent, be related to downward price pressures stemming from positive unemployment-gaps. The headline inflation rates of the remaining countries did not display persistent contributions by cyclical drivers from the early to the mid 2000s. Interestingly, the diverging country-specific contributions of unemployment balance out for the hypothetical EU10 series. This implies that fluctuations of unemployment-gaps had a limited impact on EU10 headline inflation in the early to mid 2000s (see Figure 10).

Figure 11: Actual and counter-factual inflation for the EU10 area



Overall, oil price inflation contributed little to headline inflation rates prior to the global financial crisis, but its influence has increased since 2008. It was especially important from 2014 to 2016. The increasing contribution of oil price inflation arose mainly from the decline of oil price inflation from 2014 onwards, rather than from changes of the underlying coefficient. Together, fluctuations in unemployment-gaps and oil price inflation contributed considerably to the reduction and the subsequent rise of country-specific and EU10 headline inflation rates after the start of the global financial crisis. Recently, the most debated episode of inflation dynamics is the continuous decline of headline inflation rates from 2012 to 2016, including periods of mild deflation around 2014. Our model suggests that persistently low inflation rates are the result, firstly, of slowly closing unemployment-gaps, together with a slight steepening of the Phillips curve, secondly, of a strong decrease in the oil price inflation, and, lastly, a drop in trend inflation.

To illustrate the implications of a decline in trend inflation on headline inflation in more detail, we calculate the counter-factual EU10 headline inflation from 2012m01 to 2017m03 that would have resulted if trend inflation had stayed at 1.9% (see Figure 11). The

two series indicate that the decline of trend inflation accounts for up to 0.4% of the headline inflation. By comparison, the average contributions of unemployment and oil price inflation for the EU10 area between January 2014 and April 2017 were -1% and -0.7%, respectively.

4.2 Model comparison

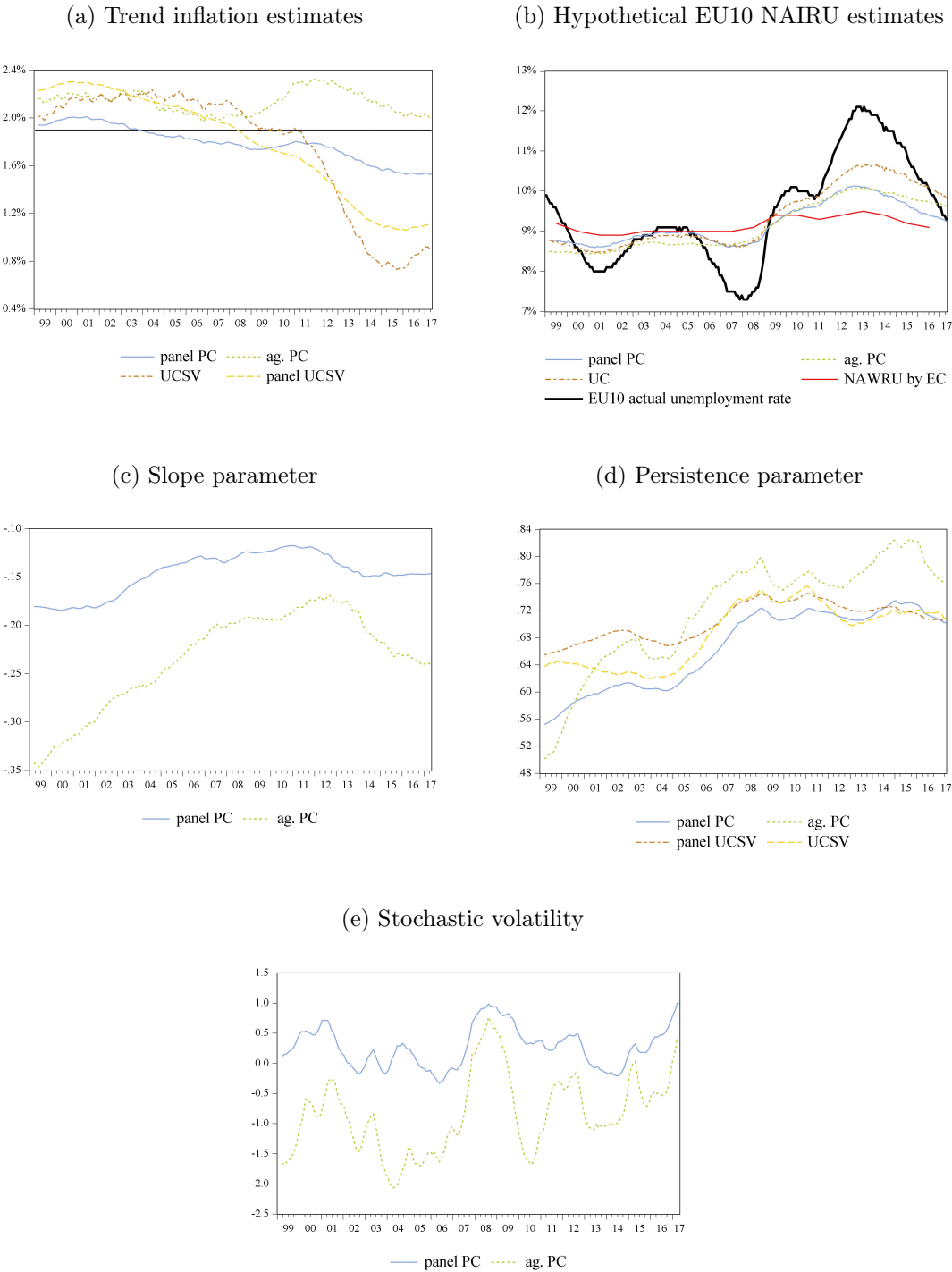
To illustrate the benefit of adding a cross-sectional dimension to the UCSV inflation model, we compare our baseline model to a variety of other aggregate, uni- and multivariate UCSV models.

Using EU10 aggregate data from January 1999 to April 2017, we estimate the plain UCSV Stock and Watson (2007) type model in inflation-gap notation denoted **UCSV**. That is a decomposition of inflation into a trend component that follows a random walk and a cyclical component that is specified as an AR(1), and the variance of residuals and the AR(1) coefficient is time-varying. Secondly, we estimate the inflation-gap Phillips curve specification similar to Stella and Stock (2013) or Chan et al. (2013) with aggregate data and augment the former model by oil price inflation. We abbreviate this model as **ag. PC**. Next, we employ a panel structure the two aforementioned models. These models are named **panel UCSV** and **panel PC**, whereby the latter version is our benchmark model. To simplify the comparison across the aggregate and panel models, we compute the hypothetical EU10 NAIRU using the country-specific posterior mean NAIRUs of the panel Phillips curve models, and country-specific weights resulting from the unemployment and labour force data. Estimation details of all models can be found in the technical appendix.

Figure 12 allows us to compare the results of our panel approach to inflation modelling along three dimensions. We can highlight the difference between panel and aggregate models, between univariate and multivariate model specification and between Phillips curve specifications. Inflation trend estimates across models (see Figure 12 Panel a) display a qualitatively similar dynamic until the start of the global financial crisis, but

diverge thereafter. Estimates by both UCSV models (**USCV** and **panel UCSV**) reveal a stronger decline of trend inflation (0.8% in 2014) than the remaining models do (1.2% in 2014).

Figure 12: Key results: comparison across models



The strong decline of trend inflation estimates in the UCSV models results from omitted additional information, since estimates of the persistence parameter and stochastic volatility in those models are similar to those of our benchmark panel PC. In the absence of additional variables that explain the inflation-gaps, the decline of both country-specific and area-wide headline inflation rates translates mainly into a decline of trend inflation. Thus, for our estimation exercise, Phillips curve models imply systematically higher trend inflation estimates, especially for the end of the sample. The estimates from the aggregate version, however, are consistently higher than those of the **panel PC** model. These estimates do not fall below 1.9% throughout the sample, and increase to 2.5% around 2012.

The higher trend inflation estimates of the aggregate model are related to systematically larger magnitude and time variation of the slope and persistence parameters, compared to the panel Phillips curve models. These larger parameter values are at odds with the empirical findings reported, for example, by Blanchard et al. (2015) and Eickmeier and Pijnenburg (2013). It is important to notice that this outcome does not hinge on distinct estimation set-ups across models, because we apply the same starting values as well as priors to panel and aggregate models. The different magnitude and time variation found may instead be a result of limited information in the time dimension of the data (17 years) for estimating slowly evolving states, which is independent of the number of observations used (our sample contains 218 observations of monthly data). As pointed out earlier, we circumvent this problem by adding a cross-sectional dimension to the model. Thus applying a panel structure results in trend estimates that decline moderately from 2013 onwards, providing much more plausible outcomes compared to survey- and market-based inflation expectations measures (see Figure 1 Panel b). Across the univariate and multivariate models, the results of the panel specifications, especially the panel Phillips curve model including oil prices, are highly plausible in economic terms.

4.3 Forecasting performance

We now examine how well our panel Phillips curve can forecast inflation since the global financial crisis. We compare the forecast performance of our baseline model to aggregate models, as well as panel UCSV and various Phillips curve models. Along similar lines as a study by Faust and Wright (2013) we also include simple autoregressive and random walk models. We perform a pseudo-out-of-sample forecast exercise for the time span January 2009 to April 2017. The models included in the forecast exercise are listed below:

- **AR(p)** with $P = 1, 2, \dots, 6$: autoregressive model for aggregate EU10 inflation following the specification of Faust and Wright (2013), $\pi_t = \phi_0 + \sum_{p=1}^P \phi_p \pi_{t-p} + \epsilon_t$
- **ARIMA(p,d,q)** with $P = 1, 2$, $D = 0$ and $Q = 1, 2$: autoregressive integrated moving average model for aggregate EU10 unemployment rate following Montgomery et al. (1998), $u_t = \sum_{p=1}^P \phi_p u_{t-p} + \epsilon_t + \sum_{q=1}^Q \theta_q \epsilon_{t-1}$
- **RW**: random walk model for aggregate EU10 inflation $\pi_t = \pi_{t-1} + \epsilon_t$
- **panel PC**: panel formulation of inflation-gap Phillips curve including oil price inflation with time-varying parameters and stochastic volatility (benchmark model)
- **panel PC excl. oil**: panel formulation of inflation-gap Phillips curve excluding oil price inflation with time-varying parameters and stochastic volatility
- **ag. PC**: aggregate inflation-gap Phillips curve including oil price inflation with time-varying parameters and stochastic volatility
- **ag. PC excl. oil**: aggregate inflation-gap Phillips curve excluding oil price inflation with time-varying parameters and stochastic volatility
- **UCSV**: unobserved component model with stochastic volatility of Stock and Watson (2007) decomposing inflation into trend and cyclical component using aggregate EU10 inflation
- **UC**: unobserved component model for EU10 aggregate unemployment with AR(2) process for unemployment-gap and a random walk process for trend unemployment.

- **panel UCSV**: panel formulation of unobserved component model with stochastic volatility
- **panel PC const. λ** : baseline model assuming that λ is constant over time
- **panel PC const. ρ** : baseline model assuming that ρ is constant over time
- **panel PC const. ω** : baseline model assuming that the oil price parameter is constant over time
- **panel PC const.:** baseline model assuming that all parameters are constant over time
- **panel PC excl. sv**: baseline model assuming that the variance of the inflation-gap equation is constant over time
- **panel PC cum. oil**: baseline model including cumulated oil price inflation (one quarter)
- **panel PC cs ρ** : baseline model allowing for country-specific persistence parameters (time-varying).

The ratios of the root mean squared forecast errors (RMSFE) of each model to the RMSFE of the AR(1) forecasts for EU10 inflation is shown in Table 1, respectively.⁴ Overall, our proposed panel structure for the Phillips curve and also for the UCSV models offers sound forecasts. For inflation forecasts from horizon 2 onwards, all our panel models outperform the aggregate uni- and multivariate models, yielding 2% to 24% smaller RMSFEs than a plain AR(1) forecast. For short-run forecasts, our benchmark model, **panel PC**, is the model that performs best. Introducing country-specific persistence in the panel Phillips curve helps to improve the short-run to mid-run (6-18 horizons) forecasts. Forecasts for 2 to 3 years ahead are predicted best by the UCSV panel model. Interestingly, the univariate AR and RW models offer better forecast performance than aggregate Phillips curves.

⁴Forecasting results for EMU unemployment rates can be found in the appendix.

Table 1: EU10 inflation: RMSFEs relative to RMSFE of the AR(1) model

model	horizon													
	1	2	4	6	9	12	15	18	21	24	27	30	33	36
AR(1)	1	1	1	1	1	1	1	1	1	1	1	1	1	1
AR(2)	1.04	1.04	1.08	1.08	1.03	1.01	1.00	1.00	1.00	0.99	1.00	0.99	0.99	0.99
AR(4)	0.92	0.98	0.99	0.98	1.00	0.99	0.99	1.00	1.00	1.00	1.00	1.00	1.00	1.01
AR(6)	0.91	0.98	1.06	1.05	1.06	1.02	1.01	1.00	1.00	0.99	1.00	0.99	0.99	0.99
RW	1.05	1.12	1.20	1.11	1.09	1.00	1.10	1.18	1.16	1.19	1.14	1.18	1.25	1.25
panel PC	1.02	0.94	0.96	0.95	0.91	0.91	0.94	0.92	0.94	0.94	0.93	0.91	0.94	0.91
panel PC excl. oil	1.02	0.95	0.98	0.97	0.95	0.97	1.01	1.00	1.01	1.02	1.02	1.00	1.02	1.01
ag. PC	1.30	1.61	1.81	1.89	1.87	1.65	1.31	1.60	1.39	0.99	1.20	1.08	0.91	1.01
ag. PC excl. oil	1.08	1.07	1.11	1.10	1.06	1.07	1.18	1.24	1.23	1.32	1.31	1.27	1.35	1.36
UCSV	1.02	1.00	1.01	0.97	0.96	0.96	1.01	1.01	1.02	1.02	1.04	1.04	1.05	1.06
panel UCSV	1.05	1.00	1.07	1.08	1.01	0.96	0.95	0.91	0.88	0.85	0.80	0.76	0.77	0.76
panel PC const. λ	1.01	0.95	0.98	0.97	0.92	0.93	0.96	0.95	0.96	0.95	0.95	0.93	0.96	0.94
panel PC const. ρ	1.00	0.95	0.99	0.97	0.93	0.94	0.98	0.97	0.95	0.95	0.96	0.94	0.95	0.92
panel PC const. σ	1.01	0.94	0.97	0.95	0.91	0.90	0.95	0.92	0.93	0.92	0.93	0.90	0.92	0.90
panel PC const. ω	1.01	0.95	0.99	0.98	0.93	0.94	0.98	0.97	0.96	0.96	0.96	0.95	0.95	0.94
panel PC excl. sv	1.03	0.95	0.99	0.96	0.92	0.90	0.94	0.91	0.91	0.91	0.92	0.87	0.90	0.87
panel PC cum. oil	1.03	0.96	0.98	0.97	0.94	0.94	0.99	0.97	0.97	0.99	0.99	0.97	0.98	0.98
panel PC cs ρ	1.03	0.96	0.97	0.94	0.90	0.88	0.94	0.92	0.92	0.92	0.91	0.90	0.91	0.91

This table displays the root mean squared forecast errors (RMSFE) of respective model relative to the RMSFE of an AR(1) model that stem from a pseudo-out-of-sample inflation forecast for the time span January 2009 to April 2017. Values lower than 1 indicate that the RMSFE of the respective model is lower than those of the AR(1) model. The results from the benchmark model are highlighted in bold. The shading indicates the respective forecasting performance, whereby green (light) shadings emphasize better forecasting performance.

5 Robustness analysis

To check the sensitivity of our baseline model, we report a series of robustness analyses in this section. The short time dimension of our sample raises the question of whether the time variation of structural parameters is a plausible assumption. Therefore, we re-estimate our benchmark model with distinct assumptions of the parameters' time variation, holding each parameter constant in turn, and then all together over time.

In addition, we leave aside the assumption on time-evolving variances of the inflation-gap residuals. Because cost-push factors might affect the inflation process with some delay, we also estimate a variant including cumulated oil price inflation (one quarter). Moreover, the identification of a Phillips curve for the EU10 area does not require the assumption of a common persistence parameter across countries. Hence, we include a model version with country-specific persistence.

Figures 13, 14 and 15 show the posterior means of the estimated states of all model variants and the benchmark specification. To summarize the country-specific NAIRU estimates, we again construct a hypothetical EU10 NAIRU for all models. All trend inflation estimates (Panel a Figure 13) depict qualitatively the same dynamics and differ to a minor extent quantitatively after the start of the sovereign debt crisis. This implies that the posterior means of the trend inflation are systematically higher for the model including cumulative oil prices, and for the model with no time variation of the oil price parameter. For those models, the posterior means of trend inflation amount to roughly 1.8% in 2016 compared to 1.6% for the benchmark model. For model variants where all parameters, only λ or only ρ_π assumed to be constant, trend inflation is lower at the end of the sample. The posterior means of the hypothetical EU10 NAIRUs display nearly no quantitative differences across models.

Turning to Figure 14, it is clear that the posterior means of the parameters display qualitatively similar dynamics. Especially the posterior means of the persistence and stochastic

Figure 13: Benchmark model and robustness specifications: posterior means of trend inflation and NAIUR

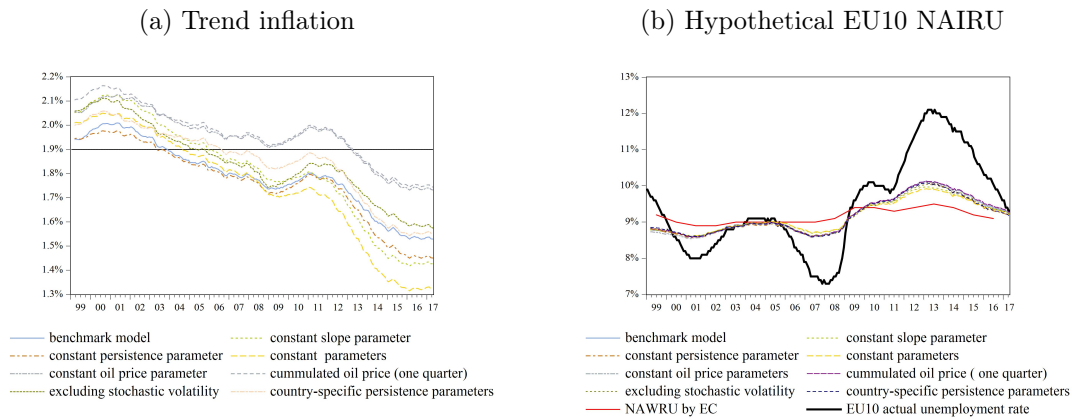
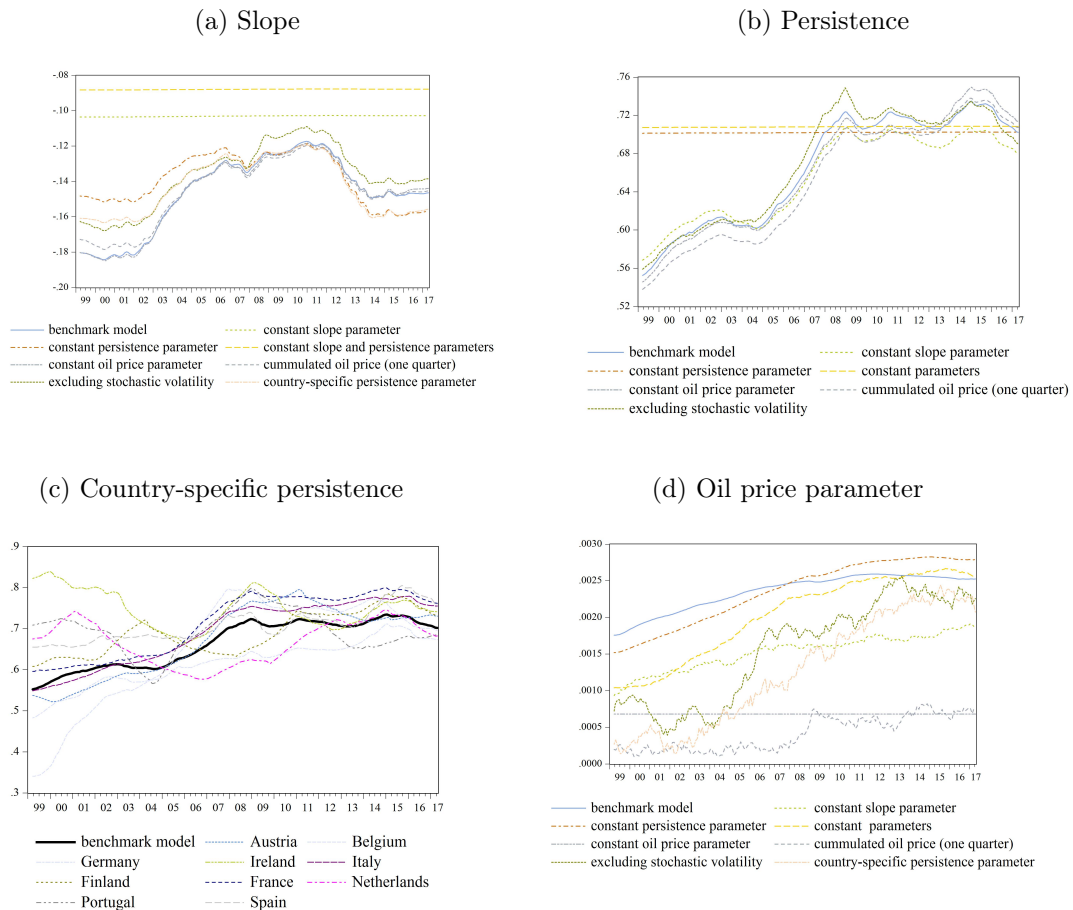
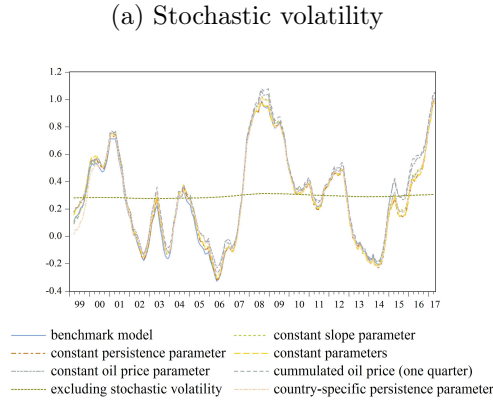


Figure 14: Benchmark model and robustness specifications: posterior means of parameters



volatility are nearly the same across models. The slope, country-specific persistence and oil price coefficients reveal some quantitative differences. Restricting the slope to be constant over time yields lower posterior means of -0.11 and -0.086 as compared to our benchmark model. Also, the model version with constant variance of the inflation-gap inflation shows

Figure 15: Benchmark model and robustness specifications: posterior mean of stochastic volatility



systematically lower evolution of the slope. Moreover, if the persistence parameter is kept constant, that leads to lower slope parameters up to the start of the global financial crisis and amplified steepening of the slope thereafter. The posterior mean of our benchmark model is around 0.6 between 1999 and 2004. Country-specific persistence estimates, however, indicate substantial differences from 1999 until 2005, with a higher degree of persistence especially for Ireland (0.8), Finland (0.7) and the Netherlands (0.68). Over time, the persistence parameters converge and deviate by roughly ± 0.05 from the benchmark model's persistence from 2008 onwards. The most pronounced difference across oil price parameters is that between the benchmark model using oil price inflation, and the version of the model using cumulated oil prices. The latter model implies a consistently lower coefficient of around 0.0003, compared to a coefficient of 0.002 in the benchmark model, but both series show a slight increase of the oil price parameter after the start of the global financial crisis. Due to the positive autocorrelation of oil price inflation, the cumulated oil price series displays altered amplitudes. As expected, this results in a lower posterior mean of the oil price parameters.

6 Conclusion

Puzzling inflation dynamics in advanced economies have been studied by a growing literature on unobserved components stochastic volatility models, thus far applied mainly

to US inflation. A prerequisite for using this type of model is a large sample that exhibits enough data variability on the time dimension. In this paper, we propose a panel non-linear UCSV Phillips curve model to investigate the inflation dynamics of the Euro area since the start of the Great Recession. We overcome the difficulty of having only limited information on the time dimension of the Euro area sample, by exploiting cross-sectional country-specific data. Our preferred panel structure for the non-linear UCSV Phillips curve model outperforms plain multivariate model versions in terms of the economic plausibility of results and in terms of forecast performance. Aggregate multivariate UCSV models indicate substantially higher trend inflation estimates and a steeper Phillips curve for the Euro area. Moreover, univariate UCSV models tend to overestimate the decline of trend inflation since 2013. These results are at odds with previous country-specific findings reported in the literature. The estimation results of our preferred model suggest that the reasons underlying the period of persistently low headline inflation in the EU10 area are threefold. Firstly, the EU10 inflation process has become more persistent in the course of the Great Recession and long-run trend inflation has significantly declined below 1.9% since 2013. According to our counter-factual analysis, this de-anchoring of inflation expectations accounted for 0.4% of headline inflation. Secondly, slowly closing unemployment-gaps, together with a slightly steeper Phillips curve exerted downward price pressure between 2013 and 2017. Lastly, the substantial fall of oil prices in 2014 amplified the decline of cyclical inflation.

References

- Anderton, R., M. Izquierdo, T. Aranki, B. Bonthuis, K. Budnik, R. Salvador, V. Jarvis, A. Lamo, A. Meyler, D. Momferatou, et al. (2012). Euro area labour markets and the crisis. Occasional Paper series 138, European Central Bank.
- Arpaia, A., A. Kiss, and A. Turrini (2014). Is unemployment structural or cyclical? main features of job matching in the eu after the crisis. Technical report, European Economy - Economic Papers 2008 - 2015.

- Autrup, S. and M. Grothe (2014). Economic surprises and inflation expectations: has anchoring of expectations survived the crisis? European Central Bank Working Paper 1671, European Central Bank.
- Ball, L. (2009). Hysteresis in unemployment. In J. Fuhrer, Y. Kodrzycki, J. Little, and G. Olivei (Eds.), *Understanding Inflation and the Implications for Monetary Policy*, Chapter 7, pp. 361–383. The MIT Press.
- Blanchard, O., E. Cerutti, and L. Summers (2015). Inflation and activity—two explorations and their monetary policy implications. NBER Working Paper 21726, National Bureau of Economic Research.
- Blinder, A. S. (2000). Central-bank credibility: Why do we care? how do we build it? *American Economic Review* 90(5), 1421–1431.
- Bobeica, E. and M. Jarocinski (2017). Missing disinflation and missing inflation: The puzzles that aren't. European Central Bank Working Paper 2000, European Central Bank.
- Chan, J. and R. Strachan (2012). Estimation in non-linear non-gaussian state space models with precision-based methods. Working Paper 39360, Munich Personal RePEc Archive.
- Chan, J. C., T. E. Clark, and G. Koop (2017). A new model of inflation, trend inflation, and long-run inflation expectations. *Journal of Money, Credit and Banking* forthcoming.
- Chan, J. C., G. Koop, and S. M. Potter (2013). A new model of trend inflation. *Journal of Business & Economic Statistics* 31(1), 94–106.
- Chan, J. C., G. Koop, and S. M. Potter (2016). A bounded model of time variation in trend inflation, nairu and the phillips curve. *Journal of Applied Econometrics* 31(3), 551–565.
- Cogley, T., G. Primiceri, and T. Sargent (2010). Inflation-gap persistence in the us. *American Economic Journal: Macroeconomics* 2(1), 43–69.

- Constâncio, Y. (2015). Understanding inflation dynamics and monetary policy. Speech at the Jackson Hole Economic Policy Symposium, European Central Bank.
- Coudert, V., C. Couharde, and V. Mignon (2013). On currency misalignments within the euro area. *Review of International Economics* 21(1), 35–48.
- Dustmann, C., B. Fitzenberger, U. Schönberg, and A. Spitz-Oener (2014). From sick man of Europe to economic superstar: Germany’s resurgent economy. *The Journal of Economic Perspectives* 28(1), 167–188.
- Eickmeier, S. and K. Pijnenburg (2013). The global dimension of inflation—evidence from factor-augmented Phillips curves. *Oxford Bulletin of Economics and Statistics* 75(1), 103–122.
- Erceg, C. J. and A. Levin (2003). Imperfect credibility and inflation persistence. *Journal of Monetary Economics* 50(4), 915–944.
- Faust, J. and J. Wright (2013). Forecasting inflation. *Handbook of economic forecasting* 2(Part A), 3–56.
- Fitzgerald, T. J., B. Holtemeyer, and J. P. Nicolini (2013, December). Is there a stable Phillips curve after all? Economic Policy Papers, Federal Reserve Bank of Minneapolis.
- Fuhrer, J., G. Olivei, and G. Tootell (2012). Inflation dynamics when inflation is near zero. *Journal of Money, Credit and Banking* 44(s1), 83–122.
- Garnier, C., E. Mertens, and E. Nelson (2015). Trend inflation in advanced economies. *International Journal of Central Banking* 11(4), 65–136.
- Greene, W. (2014). *Econometric Analysis: International Edition: Global Edition*. Pearson series in economics. Pearson Education Limited.
- Jarociński, M. and M. Lenza (2016). An inflation-predicting measure of the output gap in the euro area. Technical report, European Central Bank Working Paper No 1966.
- Matheson, T. and E. Stavrev (2013). The great recession and the inflation puzzle. *Economics Letters* 120(3), 468–472.

- Mertens, E. (2016). Measuring the level and uncertainty of trend inflation. *Review of Economics and Statistics* 98(5), 950–967.
- Montgomery, A., V. Zarnowitz, R.S.Tsay, and G. Tiao (1998). Forecasting the us unemployment rate. *Journal of the American Statistical Association* 93(442), 478–493.
- Nautz, D., L. Pagenhardt, and T. Strohsal (2017). The (de-) anchoring of inflation expectations: New evidence from the euro area. *The North American Journal of Economics and Finance* 40, 103–115.
- Paulhus, D. L. (2002). Socially desirable responding: The evolution of a construct. *The role of constructs in psychological and educational measurement* 4969, 49–69.
- Riggi, M. and F. Venditti (2015). Failing to forecast low inflation and phillips curve instability: A euro-area perspective. *International Finance* 18(1), 47–68.
- Stella, A. and J. Stock (2013). A state-dependent model for inflation forecasting. International Finance Discussion Papers 1062, Board of Governors of the Federal Reserve System.
- Stock, J. and M. Watson (2007). Why has us inflation become harder to forecast? *Journal of Money, Credit and banking* 39(1), 3–33.
- Van der Klaauw, W., W. Bruine de Bruin, G. Topa, S. Potter, and M. F. Bryan (2008). Rethinking the measurement of household inflation expectations: preliminary findings. Staff Report 359, FRB of New York.
- Watson, M. (2014). Inflation persistence, the nairu, and the great recession. *The American Economic Review* 104(5), 31–36.

7 Appendix

In this appendix we provide the details on the choice of priors and starting values as well as the MCMC-Algorithm for the estimation of the panel UCSV Phillips curve for the EU10, exploiting the cross-sectional dimension for estimating the latent states. In the first section we provide information on the model details and the prior choice. In the second section we outline the MCMC-Algorithm. In the third section we provide details on further models presented in the paper. The last section reports a prior predictive analysis.

7.1 Model and priors

Our benchmark model takes on the form:

$$\begin{aligned}
 \pi_{n,t} - \tau_t^{\pi,EU} &= \rho_t^\pi (\pi_{n,t-1} - \tau_{t-1}^{\pi,EU}) + \lambda_t (u_{n,t} - \tau_{n,t}^u) + \beta_t \pi_t^{oil} + \epsilon_{n,t}^\pi \\
 (u_{n,t} - \tau_{n,t}^u) &= \rho_{n,1}^u (u_{n,t-1} - \tau_{n,t-1}^u) + \rho_{n,2}^u (u_{n,t-2} - \tau_{n,t-2}^u) + \epsilon_{n,t}^u \\
 \tau_t^{\pi,EU} &= \tau_{t-1}^{\pi,EU} + \epsilon_t^{\tau,\pi} \\
 \tau_{n,t}^u &= \tau_{n,t-1}^u + \epsilon_{n,t}^{\tau,u} \\
 \rho_t^\pi &= \rho_{t-1}^\pi + \epsilon_t^{\rho,\pi} \\
 \lambda_t &= \lambda_{t-1} + \epsilon_t^\lambda \\
 \beta_t &= \beta_{t-1} + \epsilon_t^\beta
 \end{aligned} \tag{3}$$

with $n = 1, \dots, N$ number of countries, $t = 1, \dots, T$ points in time and

$$\begin{aligned}
\epsilon_{n,t}^\pi &\sim N(0, e^{h_t}) \\
h_t &= h_{t-1} + \epsilon_t^h \\
\epsilon_t^h &\sim N(0, \sigma_h^2) \\
\epsilon_{n,t}^u &\sim N(0, \sigma_{n,u}^2) \\
\epsilon^{\rho^\pi} &\sim TN(-\rho_{t-1}^\pi, 1 - \rho_{t-1}^\pi; 0, \sigma_{\rho^\pi}^2) \\
\epsilon^\lambda &\sim TN(-1 - \lambda_{t-1}, 0 - \lambda_{t-1}; 0, \sigma_\lambda^2) \\
\epsilon^\beta &\sim TN(-\beta_{t-1}, 1 - \beta_{t-1}; 0, \sigma_\beta^2)
\end{aligned} \tag{4}$$

Moreover, we impose that the unemployment-gaps evolve as a stationary AR(2) process, restricting $\rho_{n,1}^u + \rho_{n,2}^u < 1$, $\rho_{n,2}^u - \rho_{n,1}^u < 1$ and $|\rho_{n,2}^u| < 1$. Additionally, we assume that λ_t , ρ_t^π and β_t lie in the intervals $(-1, 0)$, $(0, 1)$ and $(0, 1)$, respectively. The prior for initial conditions of the state equations are

$$\begin{aligned}
\tau_1^{\pi,EU} &\sim N(\tau_0^{\pi,EU}, \omega_{\tau^\pi}^2) \\
\tau_{n,1}^u &\sim N(\tau_{n,0}^u, \omega_{\tau^u}^2) \\
\rho_1^\pi &\sim TN(0, 1; \rho_0^\pi, \omega_{\rho^\pi}^2) \\
\lambda_1 &\sim TN(-1, 0; \lambda_0, \omega_\lambda^2) \\
\beta_1 &\sim TN(0, 1; \beta_0, \omega_\beta^2) \\
h_1 &\sim TN(h_0, \omega_h^2)
\end{aligned}$$

whereby $\tau_0^{\pi,EU}$, $\tau_{n,0}^u$, ρ_0^π , λ_0 , β_0 , h_0 , $\omega_{\tau^\pi}^2$, $\omega_{\tau^u}^2$, $\omega_{\rho^\pi}^2$, ω_λ^2 , ω_β^2 and ω_h^2 are known constants. The

specific choice of initial conditions are shown in table 2. For the model parameters we choose the following priors

$$\begin{aligned}
\sigma_{u,n}^2 &\sim IG(\underline{v}_u, \underline{S}_u) \\
\sigma_h^2 &\sim IG(\underline{v}_h, \underline{S}_h) \\
\sigma_{\tau^\pi}^2 &\sim IG(\underline{v}_{\tau^\pi}, \underline{S}_{\tau^\pi}) \\
\sigma_{\tau^u,n}^2 &\sim IG(\underline{v}_{\tau^u,n}, \underline{S}_{\tau^u,n}) \\
\sigma_{\rho^\pi}^2 &\sim IG(\underline{v}_{\rho^\pi}, \underline{S}_{\rho^\pi}) \\
\sigma_\lambda^2 &\sim IG(\underline{v}_\lambda, \underline{S}_\lambda) \\
\sigma_\beta^2 &\sim IG(\underline{v}_\beta, \underline{S}_\beta)
\end{aligned}$$

IG denotes the inverse-Gamma distribution. The initial values and priors are shown in table 2. The prior for the degrees of freedom for the parameters is small as $v = 10$, implying a large variance and therewith a relatively non-informative prior. The scale parameters are set in way as to reflect the desired smoothness of tvp parameters and trends in terms of expected value of the respective variances. For example $S_{\tau^\pi} = 0.9$ with $E(\sigma_{\tau^\pi}) = 0.1$ then the prior for $E(\sigma_{\tau^\pi})$ implies a relatively smooth transition of τ^π . With a high probability τ^π changes between -0.01 and 0.01 from one period to another. Since the inflation trend is common across countries but the unemployment trend is country-specific we employ distinct scale parameters for the unemployment trends, reflecting differences across country-specific NAIRUs due to structural differences across labour markets.

7.2 MCMC sampling

We adapt the algorithm introduced by Chan et al. (2016) and sequentially draw from

1. $p(\tau^{\pi,EU} | \pi, u, \tau^u, \rho^\pi, \lambda, \beta, h, \theta, IV)$
2. $p(\tau^u | \pi, u, \tau^{\pi,EU}, \rho^\pi, \lambda, \beta, h, \theta, IV)$

Table 2: Initial conditions and priors

Initial conditions:											
τ_0^π	τ_0^u										h_0
1.9	OE	BG	BD	ES	FN	FR	IR	IT	NL	PT	1
ρ_0^π	λ_0	β_0	$\rho_{1,0}^u$	$\rho_{2,0}^u$	$\omega_{\tau^\pi}^2$	$\omega_{\tau^u}^2$	ω_h^2	$\omega_{\rho^\pi}^2$	ω_λ^2	ω_β^2	ω_u^2
0.7	-0.4	0.001	1.6	-0.7	0.01	0.1	0.2	0.005	0.005	10^{-8}	0.2
Priors											
\underline{S}_{τ^π}	\underline{S}_{τ^u}										\underline{S}_h
0.9	OE	BG	BD	ES	FN	FR	IR	IT	NL	PT	1.8
0.9	0.9	0.9	0.9	3.6	1.8	0.9	4.5	0.9	1.8	0.9	1.8
\underline{S}_u	\underline{S}_{ρ^π}	\underline{S}_λ	\underline{S}_β	For σ^2 of τ^π , τ^u , h , ρ^π , λ and β we set \underline{v}							
4.5	0.081	0.081	$4.5e^{-6}$	10							

$$3. p(\rho^\pi | \pi, u, \tau^{\pi, EU}, \tau^u, \lambda, \beta, h, \theta, IV)$$

$$4. p(\lambda | \pi, u, \tau^{\pi, EU}, \tau^u, \rho^\pi, \beta, h, \theta, IV)$$

$$5. p(\beta | \pi, u, \tau^{\pi, EU}, \tau^u, \rho^\pi, \lambda, h, \theta, IV)$$

$$6. p(h | \pi, u, \tau^{\pi, EU}, \tau^u, \rho^\pi, \lambda, \beta, \theta, IV)$$

$$7. p(\theta | \pi, u, \tau^{\pi, EU}, \tau^u, \rho^\pi, \lambda, \beta, h, IV)$$

with $\theta = (\sigma_u, \sigma_{\tau^{\pi, EU}}, \sigma_{\tau^u}, \sigma_h, \sigma_{\rho^\pi}, \sigma_\lambda, \sigma_\beta, \rho^u)$ and IV being the initial values for the respective parameters.

Conditional distribution of $\tau^{\pi, EU}$

To obtain the conditional distribution of $\tau^{\pi, EU}$ we rewrite the inflation equation in the following way:

$$K_\pi \pi = \mu_\pi + K_\pi X_0 \tau^{\pi, EU} + \epsilon^\pi, \quad \epsilon^\pi \sim N(0, \Omega_\pi) \quad (5)$$

whereby π is $NT \times 1$, $\tau^{\pi, EU}$ is $T \times 1$, $\epsilon_{n,T}^\pi$ is $NT \times 1$, Ω_π is $\text{diag}(\sigma_{1,1}^2, \dots, \sigma_{N,1}^2, \dots, \sigma_{N,T}^2)$ and

$$K_\pi = \begin{bmatrix} I_N & 0 & 0 & 0 \\ -\rho_2^\pi I_N & I_N & 0 & 0 \\ 0 & -\rho_2^\pi I_N & I_N & 0 \\ \vdots & \dots & \ddots & \vdots \\ 0 & 0 & 0 & -\rho_2^\pi I_N \end{bmatrix}$$

$NT \times NT$

I_N is an identity matrix of $N \times N$. Since $|K| = 1$, K_π is invertible for all values of ρ^π

$$\mu_\pi = \begin{bmatrix} \rho_1^\pi(\pi_{1,0} - \tau^{\pi, EU}) + \lambda_1(u_{1,1} - \tau_{1,1}^u) + \beta_1 \pi_1^{oil} \\ \rho_1^\pi(\pi_{N,0} - \tau^{\pi, EU}) + \lambda_1(u_{N,1} - \tau_{N,1}^u) + \beta_1 \pi_1^{oil} \\ \lambda_2(u_{1,2} - \tau_{1,2}^u) + \beta_2 \pi_2^{oil} \\ \vdots \\ \lambda_2(u_{N,2} - \tau_{N,2}^u) + \beta_2 \pi_2^{oil} \\ \vdots \\ \lambda_T(u_{N,T} - \tau_{N,T}^u) + \beta_T \pi_T^{oil} \end{bmatrix}$$

$NT \times 1$

$$X_0 = \begin{bmatrix} \iota & \dots & \dots & \dots & \dots & 0 \\ 0 & \iota & \dots & \dots & \dots & \vdots \\ 0 & 0 & \iota & \dots & \dots & \vdots \\ \vdots & \dots & \dots & \ddots & \dots & \vdots \\ 0 & \dots & \dots & \dots & \dots & \iota \end{bmatrix}$$

$NT \times T$

ι as a column vector of $N \times 1$ ones. Note that $(X_0' X_0)$ is an invertible $NT \times NT$ matrix.

$$(M\pi|u, \tau^u, \rho^\pi, \rho^u, \lambda, \beta, h, \theta) \sim N(MK_\pi^{-1}\mu_\pi + X_0\tau^{\pi, EU}, (M'K_\pi'^{-1}\Omega_\pi K^{-1}M)) \quad (6)$$

whereby $M = (X_0' X_0)^{-1} X_0'$. Then the prior density of $M\pi$ is given by

$$\begin{aligned} \log p(M\pi|u, \tau^u, \rho^\pi, \rho^u, \lambda, \beta, h, \theta) \propto \\ -\frac{1}{2}jh - \frac{1}{2}(M\pi - MK_\pi^{-1}\mu_\pi - \tau^{\pi, EU})'(M'K_\pi'^{-1}\Omega_\pi K^{-1}M)^{-1} \\ (M\pi - MK_\pi^{-1}\mu_\pi - \tau^{\pi, EU}) \end{aligned} \quad (7)$$

with j being a $NT \times 1$ columns of ones. The state equation of $\tau^{\pi,EU}$ is defined as

$$H\tau^{\pi,EU} = \alpha_\pi + \epsilon^{\tau\pi} \quad (8)$$

with

$$\alpha_\pi = \begin{bmatrix} \tau_0^{\pi,EU} \\ 0 \\ \vdots \\ 0 \end{bmatrix} \quad H = \begin{bmatrix} 1 & 0 & 0 & \dots & \dots & 0 \\ -1 & 1 & 0 & \dots & \dots & \vdots \\ 0 & -1 & 1 & \dots & \dots & \vdots \\ 0 & 0 & -1 & 1 & \dots & \vdots \\ \vdots & \dots & \dots & \dots & \ddots & \vdots \\ 0 & 0 & \dots & \dots & -1 & 1 \end{bmatrix}$$

so that

$$(\tau^{\pi,EU} | \sigma_{\tau,\pi}^2) \sim N(H^{-1}\alpha_\pi, (H'\Omega_{\tau\pi}^{-1}H)^{-1}) \quad (9)$$

with $\Omega_{\tau\pi} = \text{diag}(\omega_{\tau\pi}^2, \sigma_{\tau\pi}^2, \dots, \sigma_{\tau\pi}^2)$. The prior density of $\tau^{\pi,EU}$ is given by

$$\begin{aligned} \log p(\tau^{\pi,EU} | \sigma_{\tau,\pi}^2) &\propto \\ &-\frac{1}{2}(\tau^{\pi,EU} - H^{-1}\alpha_\pi)' H' \Omega_{\tau\pi}^{-1} H (\tau^{\pi,EU} - H^{-1}\alpha_\pi) \end{aligned} \quad (10)$$

Combining (7) and (10)

$$\begin{aligned} \log p(\tau^{\pi,EU} | M\pi, u, \tau^u, \rho^\pi, \lambda, \beta, h, \theta) &\propto \\ &-\frac{1}{2}(\tau^\pi - \hat{\tau}^\pi)' D_{\tau,\pi}^{-1} (\tau^\pi - \hat{\tau}^\pi) \end{aligned} \quad (11)$$

with

$$\begin{aligned} \hat{\tau}^{\pi,EU} &= D_{\tau,\pi}((M'K_\pi'^{-1}\Omega_\pi K_\pi^{-1}M)^{-1}(M\pi - MK_\pi^{-1}\mu_\pi) + H'\Omega_{\tau\pi}^{-1}\alpha_\pi) \\ D_{\tau,\pi} &= ((M'K_\pi'^{-1}\Omega_\pi K_\pi^{-1}M)^{-1} + H'\Omega_{\tau\pi}^{-1}H)^{-1} \end{aligned}$$

We sample $N(\hat{\tau}^{\pi,EU}, D_{\tau,\pi})$ by using the precision-based-algorithm developed by Chan and Jeliazkov (2009). This implies that we sample $\hat{\tau}^{\pi,EU}$ by applying the Cholesky factorisation to $D_{\tau,\pi}$ that is a block-banded matrix so that $C'C = D_{\tau,\pi}$. Then we solve for $\hat{\tau}^{\pi,EU}$ by backward and forward substitution, sample $u \propto N(0, I)$, solve for $Cx = u$ and get a draw of $\tau^{\pi,EU}$ by $\tau^{\pi,EU} = \hat{\tau}^{\pi,EU} + x$ with $\tau^{\pi,EU} \propto N(\hat{\tau}^{\pi,EU}, D_{\tau,\pi})$.

Conditional distribution of τ^u

Next we derive the conditional distribution of τ^u . Therefore, we rewrite the Phillips curve equation as

$$z = \Lambda\tau^u + \epsilon^\pi, \quad \epsilon^\pi \sim N(0, \Omega_\pi) \quad (12)$$

with

$$z = \begin{bmatrix} (\pi_{1,1} - \tau_1^{\pi,EU}) - \rho_{1,1}^\pi(\pi_{1,0} - \tau_0^{\pi,EU}) - \lambda_1 u_{1,1} - \beta_1 \pi_1^{oil} \\ \vdots \\ (\pi_{N,1} - \tau_1^{\pi,EU}) - \rho_{N,1}^\pi(\pi_{N,0} - \tau_0^{\pi,EU}) - \lambda_1 u_{N,1} - \beta_1 \pi_1^{oil} \\ (\pi_{N,T} - \tau_T^{\pi,EU}) - \rho_{N,T}^\pi(\pi_{N,T-1} - \tau_{T-1}^{\pi,EU}) - \lambda_T u_{N,T} - \beta_T \pi_T^{oil} \end{bmatrix}$$

$$\Lambda = \text{diag}(-\lambda_{1,1}, \dots, -\lambda_{N,1}, \dots, -\lambda_{N,T})$$

$$\tau^u = [\tau_{1,1}^u, \dots, \tau_{N,1}^u, \dots, \tau_{N,T}^u]'$$

The prior density of π is then given by

$$\log p(\pi|u, \tau^u, \tau^\pi, \rho^\pi, \lambda, \beta, h, \theta) \propto (z - \Lambda\tau^u)' \Omega_\pi^{-1} (z - \Lambda\tau^u) \quad (13)$$

The second measurement equation for τ^u stems from the unemployment-gap formulation.

$$K_u u = \mu_u + K_u \tau^u + \epsilon^u, \quad \epsilon^u \sim N(0, \Omega_u) \quad (14)$$

with $\Omega_u = I_T \otimes \sigma_u^2$, $\sigma_u^2 = [\omega_u^2, \sigma_{1,u}^2, \dots, \sigma_{N,u}^2]'$ and

$$\mu_u = \begin{bmatrix} \rho_{1,1}^u(u_{1,0} - \tau_{1,0}^u) + \rho_{1,2}^u(u_{1,-1} - \tau_{1,-1}^u) \\ \vdots \\ \rho_{N,1}^u(u_{N,0} - \tau_{N,0}^u) + \rho_{N,2}^u(u_{N,-1} - \tau_{N,-1}^u) \\ \vdots \\ \rho_{1,2}^u(u_{1,0} - \tau_{1,0}^u) \\ \vdots \\ \rho_{N,2}^u(u_{N,0} - \tau_{N,0}^u) \\ \vdots \\ 0 \end{bmatrix}$$

$$K_u = \begin{bmatrix} I_N & 0 & \dots & \dots & \dots & 0 \\ -\rho_1^u I_N & I_N & \dots & \dots & \dots & \dots \\ -\rho_2^u I_N & -\rho_1^u I_N & I_N & \dots & \ddots & \vdots \\ 0 & -\rho_2^u I_N & -\rho_1^u I_N & I_N & \dots & \vdots \\ \vdots & \dots & \dots & \dots & \ddots & \vdots \\ 0 & \dots & \dots & -\rho_2^u I_N & -\rho_1^u I_N & I_N \end{bmatrix}$$

whereby ρ_1^u and ρ_2^u are column vectors with $1 \times N$.

The prior density of u is then given by

$$\log p(u|\tau^u, \theta) \propto -\frac{1}{2}(u - K_u^{-1}\mu_u - \tau^u)' K_u' \Omega_u^{-1} K_u (u - K_u^{-1}\mu_u - \tau^u) \quad (15)$$

The state equation τ^u takes on the form

$$\tau^u = H^{-1}\alpha_u + \epsilon_t^{\tau^u} \quad (16)$$

with $\alpha_u = (\tau_0^u, \dots, 0)'$ and $\Omega_{\tau^u} = \text{diag}(\omega_{\tau^u}^2, \sigma_{\tau^u}^2, \dots, \sigma_{\tau^u}^2)$

$$\log p(\tau^u|\sigma_{\tau^u}^2) \propto -\frac{1}{2}(\tau^u - H^{-1}\alpha_u)' H' \Omega_{\tau^u}^{-1} H (\tau^u - H^{-1}\alpha_u) \quad (17)$$

Next, combining (13), (15) and (17) yields

$$\begin{aligned}
\log p(\tau^u | \pi, u, \rho^\pi, \tau^\pi, \lambda, \beta, h, \theta) &\propto \\
&-\frac{1}{2}(z - \Lambda\tau^u)' \Omega_\pi^{-1} (z - \Lambda\tau^u) \\
&-\frac{1}{2}(u - K_u^{-1}\mu_u - \tau^u)' K_u' \Omega_u^{-1} K_u (u - K_u^{-1}\mu_u - \tau^u) \\
&-\frac{1}{2}(\tau^u - H^{-1}\alpha_u)' H' \Omega_{\tau^u}^{-1} H (\tau^u - H^{-1}\alpha_u) \\
&= -\frac{1}{2}(\tau^u - \hat{\tau}^u)' D_{\tau^u} (\tau^u - \hat{\tau}^u)
\end{aligned}$$

with

$$\hat{\tau}^u = D_{\tau^u} (\Lambda' \Omega_\pi^{-1} z + K_u' \Omega_u^{-1} K_u (u - K_u^{-1} \mu_u) + H' \Omega_{\tau^u}^{-1} \alpha_u) \quad (18)$$

$$D_{\tau^u} = (\Lambda' \Omega_\pi^{-1} \Lambda + K_u' \Omega_u^{-1} K_u + H' \Omega_{\tau^u}^{-1} H)^{-1} \quad (19)$$

As before we sample the distribution by using the precision-based algorithm.

Conditional distribution of ρ^π

The measurement equation for ρ_π is

$$\pi^* + \Lambda u^* + \beta_t \pi_t^{oil} = X_\pi X_0 \rho^\pi + \epsilon^\pi \quad (20)$$

whereby $\pi^* = \pi - X_0 \tau^{\pi, EU}$, $X_\pi = \text{diag}(\pi_0^*, \dots, \pi_{N, T-1}^*)$, $\rho^\pi = [\rho_0^\pi, \rho_1^\pi, \dots, \rho_T^\pi]'$ and $u^* = u - \tau^u$. Then it follows that

$$(M X_\pi^{-1} \pi^* + M X_\pi^{-1} \Lambda u^*) \sim N(\rho^\pi, M' X_\pi'^{-1} \Omega_\pi X_\pi^{-1} M) \quad (21)$$

$$\begin{aligned}
\log p(MX_\pi^{-1}\pi^* + MX_\pi^{-1}\Lambda u^* | \tau^\pi, \tau^u, \rho^\pi, \lambda, \beta, h, \theta) \propto & \\
& -\frac{1}{2}j_T h - \frac{1}{2}(MX_\pi^{-1}\pi^* + MX_\pi^{-1}\Lambda u^* - \rho^\pi)' \\
& (MX_\pi^{-1}\Omega_\pi X_\pi'^{-1}M')^{-1} \\
& (MX_\pi^{-1}\pi^* + MX_\pi^{-1}\Lambda u^* - \rho^\pi)
\end{aligned} \tag{22}$$

The state equation of ρ_π is given by

$$H\rho^\pi = \epsilon^{\rho^\pi}, \quad \rho^\pi \sim N(0, H'^{-1}\Omega_{\rho^\pi}H^{-1}) \tag{23}$$

with

$$\begin{aligned}
\log p(\rho^\pi | \sigma_{\rho^\pi}^2) \propto & \\
& -\frac{1}{2}(\rho^{\pi'} H' \Omega_{\rho^\pi}^{-1} H \rho^\pi) + g_{\rho^\pi, \sigma_{\rho^\pi}^2}
\end{aligned} \tag{24}$$

Combining (22) and (24) yields

$$\begin{aligned}
\log p(\rho^\pi | \pi, u, \tau^\pi, \tau^u, \lambda, \beta, h, \theta) \propto & \\
& -\frac{1}{2}j_T h - \frac{1}{2}(MX_\pi^{-1}\pi^* + MX_\pi^{-1}\Lambda u^* - \rho^\pi)'(MX_\pi^{-1}\Omega_\pi X_\pi'^{-1}M')^{-1} \\
& (MX_\pi^{-1}\pi^* + MX_\pi^{-1}\Lambda u^* - \rho^\pi) \\
& -\frac{1}{2}(\rho^{\pi'} H' \Omega_{\rho^\pi}^{-1} H \rho^\pi) + g_{\rho^\pi, \sigma_{\rho^\pi}^2} \\
\propto & -\frac{1}{2}(\rho^\pi - \hat{\rho}^\pi)' D_{\rho^\pi}^{-1} (\rho^\pi - \hat{\rho}^\pi) + g_{\rho^\pi, \sigma_{\rho^\pi}^2}
\end{aligned} \tag{25}$$

with

$$g_{\rho^\pi, \sigma_{\rho^\pi}^2} = -\sum_{t=2}^T \left(\Phi\left(\frac{1-\rho_{t-1}^\pi}{\sigma_{\rho^\pi}^2}\right) - \Phi\left(\frac{-\rho_t^\pi}{\sigma_{\rho^\pi}^2}\right) \right)$$

$$\begin{aligned}\hat{\rho}^\pi &= D_{\rho^\pi}((M'X_\pi'^{-1}\Omega_\pi X_\pi^{-1}M)^{-1}MX_\pi^{-1}(\pi^* + \Lambda u^*)) \\ D_{\rho^\pi} &= ((M'X_\pi'^{-1}\Omega_\pi X_\pi^{-1}M)^{-1} + H'\Omega_{\rho^\pi}^{-1}H)^{-1}\end{aligned}$$

As it can be seen in EQ (25) the conditional density for ρ^π is truncated-normal. We follow Chan et al. (2016) and apply an independence chain Metropolis-Hastings step, whereby the candidate draws resulting from the precision-based method are accepted or rejected by an acceptance-rejection Metropolis-Hastings step.

Conditional distribution of λ

The measurement equation of λ takes on the following form

$$\pi_\lambda = X_u X_0 \lambda + \epsilon^\pi \quad (26)$$

with $X_u = \text{diag}(u_{1,0}^*, \dots, u_{N,T-1}^*)$ and $\pi_\lambda = [\pi_{1,1}^* - \rho_1^\pi \pi_{1,0}^* - \beta_1 \pi_1^{oil}, \dots, \pi_{N,1}^* - \rho_1^\pi \pi_{N,0}^* - \beta_1 \pi_1^{oil}, \dots, \pi_{N,T}^* - \rho_T^\pi \pi_{N,T-1}^* - \beta_T \pi_T^{oil}]'$. Then it follows that

$$MX_u^{-1}w \sim N(\lambda, M'X_u'^{-1}\Omega_\pi X_u^{-1}M) \quad (27)$$

with

$$\begin{aligned}\log p(MX_u^{-1}\pi_\lambda | \tau^\pi, \tau^u, \rho^\pi, \lambda, \beta, h, \theta) \propto \\ -\frac{1}{2}j_T h - \frac{1}{2}(MX_u^{-1}\pi_\lambda - \lambda)'(MX_u^{-1}\Omega_\pi X_u'^{-1}M)^{-1} \\ (MX_u^{-1}\pi_\lambda - \lambda)\end{aligned} \quad (28)$$

The state equation of λ is given by

$$H\lambda = \epsilon_t^\lambda, \quad \epsilon_t^\lambda \sim N(0, \Omega_\lambda) \quad (29)$$

with

$$\begin{aligned} \log p(\lambda|\sigma_\lambda^2) &\propto \\ &-\frac{1}{2}(\lambda)'H'\Omega_\lambda^{-1}H(\lambda) + g_\lambda(\lambda, \sigma_\lambda^2) \end{aligned} \quad (30)$$

Combining (28) and (30) yields

$$\begin{aligned} \log p(\lambda|\pi, u, \tau^\pi, \tau^u, \rho^\pi, \beta, h, \theta) &\propto \\ &-\frac{1}{2}(\lambda - \hat{\lambda})'D_\lambda^{-1}(\lambda - \hat{\lambda}) + g_\lambda \end{aligned} \quad (31)$$

with

$$\begin{aligned} g_\lambda(\lambda, \sigma_\lambda^2) &= -\sum_{t=2}^T (\Phi(\frac{-\lambda_{t-1}}{\sigma_\lambda} - \Phi(\frac{-1-\lambda}{\sigma_\lambda})) \\ \hat{\lambda} &= D_\lambda((MX_u^{-1}\Omega_\pi X_u'^{-1}M')^{-1}MX_u^{-1}\pi_\lambda) \\ D_\lambda &= ((MX_u^{-1}\Omega_\pi X_u'^{-1}M')^{-1} + H'\Omega_\lambda^{-1}H)^{-1} \end{aligned}$$

Similarly to the sampling of ρ^π , we include an acceptance-rejection Metropolis-Hastings (ARMH) step additional to the precision-based algorithm as the conditional density is of non-standard form.

Conditional distribution of β

We apply a similar derivation strategy as before. Then the measurement equation of β takes on the following form

$$\pi_{oil}^* = X_0 X_{oil} \beta + \epsilon^\pi \quad (32)$$

with $X_{oil} = \text{diag}(\pi_1^{oil}, \dots, \pi_T^{oil})$, $\beta = [\beta_0, \beta_1, \dots, \beta_T]'$ and $\pi_{oil}^* = [\pi_{1,1} - X_0 \tau_1^{\pi, EU} - \rho_1^\pi (\pi_{1,0} - X_0 \tau_0^{\pi, EU}) - \lambda_1 u_{1,1}^*, \dots, \pi_{N,1} - X_0 \tau_1^{\pi, EU} - \rho_1^\pi (\pi_{N,0} - X_0 \tau_0^{\pi, EU}) - \lambda_1 u_{N,1}^*, \dots, \pi_{N,T} - X_0 \tau_T^{\pi, EU} - \rho_T^\pi (\pi_{N,T-1} - X_0 \tau_{T-1}^{\pi, EU} - 1) - \lambda_T u_{N,T}^*]'$. Then it follows that

$$\begin{aligned} \log p(X_{oil}^{-1}Md|\tau^\pi, \tau^u, \rho^\pi, \lambda, h, \theta) &\propto \\ &-\frac{1}{2}j_T h - \frac{1}{2}(X_{oil}^{-1}Md - \beta)'(X_{oil}^{\prime-1}M'\Omega_{oil}MX_{oil}^{-1})^{-1} \\ &(X_{oil}^{-1}Md - \beta) \end{aligned} \quad (33)$$

The state equation of β is given by

$$H\beta = \epsilon_t^\beta, \quad \epsilon_t^\beta \sim N(0, \Omega_\beta) \quad (34)$$

with

$$\begin{aligned} \log p(\beta|\sigma_\beta^2) \propto & \\ & -\frac{1}{2}(\beta)'H'\Omega_\beta^{-1}H(\beta) + g_\beta(\beta, \sigma_\beta^2) \end{aligned} \quad (35)$$

Combining (33) and (35) yields

$$\begin{aligned} \log p(\beta|\pi, u, \tau^\pi, \tau^u, \rho^\pi, \beta, h, \theta) \propto & \\ & -\frac{1}{2}(\beta - \hat{\beta})'D_\beta^{-1}(\beta - \hat{\beta}) + g_\beta \end{aligned} \quad (36)$$

with

$$\begin{aligned} g_{\beta, \sigma_\beta^2} &= -\sum_{t=2}^T \left(\Phi\left(\frac{1-\beta_{t-1}}{\sigma_\beta^2}\right) - \Phi\left(\frac{-\beta}{\sigma_\beta^2}\right) \right) \\ \hat{\beta} &= D_\beta(X'_{oil}M'^{-1}\Omega_\beta^{-1}\pi_{oil}^*) \\ D_\beta &= (X'_{oil}M'^{-1}\Omega_\beta^{-1}M^{-1}X_{oil} + H'\Omega_\beta^{-1}H)^{-1} \end{aligned}$$

As before we include an acceptance-rejection Metropolis-Hastings (ARMH) step additional to the precision-based algorithm as the conditional density is of non-standard form.

Sampling h and θ

For sampling h and the remaining parameters summarized by θ we stick to the algorithm developed by Chan and Strachan (2012) that is also used in Chan et al. (2016). Thereby, we draw ρ^u from a bivariate truncated normal distribution, employing an ARMH step. Moreover, we draw all remaining variances in separate blocks from inverse-Gamma distributions. We refer the reader to Chan and Strachan (2012) and Chan et al. (2016) for further technical details.⁵

⁵It should be noted that we do not bound $\tau^{\pi, EU}$ nor τ^u as in Chan et al. (2016).

7.3 Specifications of other models

We now report details on the additional unobserved component models presented in the model comparison and forecasting exercise in the paper. The algorithm underlying these models are in principle variants of the algorithm presented in the previous section and are very close to those of Chan et al. (2013) and Chan et al. (2016). For all model variants that differ with respect to the time variation of parameters we employ the settings as presented in table 2 and just switch off the respective state equation(s). Similarly, for the PC variants that do not include oil prices we set the same starting values and priors for the panel PC model as in table 2 and for the aggregate PC model as described below. Thus, in the remainder of this section we focus on the univariate unobserved component models and the aggregate Phillips curve model. Turning first to the univariate models, the **UCSV**, **panel UCSV** and **UC** model take on the following forms stated below.

For comparability across models we employ similar priors and starting values as in our benchmark specification. Thus, for panel and aggregate, UCSV models we set $\tau_0^\pi = \tau_0^{\pi,EU} = 1.9$, $\rho_0^\pi = 0.7$, $h_0 = 1$, $\omega_{\tau,\pi}^2 = 0.01$, $\omega_{\rho,\pi}^2 = 0.005$, $\omega_h^2 = 0.2$. As before we specify the model parameters as inverse-Gamma distributions so that for $\sigma_{\tau,\pi}^2$, $\sigma_{\rho,\pi}^2$ and σ_h^2 we have $\sigma^2 \sim IG(\underline{v}, \underline{S})$. We set $v_h = v_\tau = v_{\rho,\pi} = 10$, $S_h = 1.8$, $S_\tau = 0.9$ and $S_{\rho,\pi} = 0.81$. The starting values for the UC model are $\tau_0^u = [9, 9]$, $\rho_{1,0}^u = 1.6$, $\rho_{2,0}^u = -0.7$, $\omega_u^2 = 0.2$ and $\omega_{\tau^u}^2 = 0.01$. We again assume that σ_u^2 and $\sigma_{\tau^u}^2$ follow an inverse-Gamma distribution and set $v_{\tau^u} = v_u = 10$ and $S_{\tau^u} = 3.6$. For the aforementioned models ρ^π and ρ^u stem from truncated normal distributions as detailed in the benchmark model specification.

The multivariate but aggregate Phillips curve model is specified below. Model parameters are again specified as inverse-Gamma distributions and we apply the same starting values as well as priors as in our baseline model (see table 2), except for τ_0^u and S_{τ^u} , which we set to $[9; 9]$ and 3.6, respectively.

UCSV

$$\pi_t - \tau_t^\pi = \rho_t^\pi (\pi_{t-1} - \tau_{t-1}^\pi) + \epsilon_t^\pi$$

$$\tau_t^\pi = \tau_{t-1}^\pi + \epsilon_t^{\tau,\pi}$$

$$\rho_t^\pi = \rho_{t-1}^\pi + \epsilon_t^{\rho,\pi}$$

$$\epsilon_t^\pi \sim N(0, e^{h_t})$$

$$h_t = h_{t-1} + \epsilon_t^h$$

$$\epsilon_t^h \sim N(0, \sigma_h^2)$$

$$\epsilon^{\rho^\pi} \sim TN(-\rho_{t-1}^\pi, 1 - \rho_{t-1}^\pi; 0, \sigma_{\rho^\pi}^2)$$

UC

$$u_t - \tau_t^u = \rho_1^u (u_{t-1} - \tau_{t-1}^u) + \rho_2^u (u_{t-2} - \tau_{t-2}^u) + \epsilon_t^u$$

$$\tau_t^u = \tau_{t-1}^u + \epsilon_t^{\tau^u}$$

$$\epsilon_t^u \sim N(0, \sigma_u^2)$$

panel UCSV

$$\pi_{n,t} - \tau_t^{\pi,EU} = \rho_t^\pi (\pi_{n,t-1} - \tau_{t-1}^{\pi,EU}) + \epsilon_{n,t}^\pi$$

$$\tau_t^{\pi,EU} = \tau_{t-1}^{\pi,EU} + \epsilon_t^{\tau,\pi}$$

$$\rho_t^\pi = \rho_{t-1}^\pi + \epsilon_t^{\rho,\pi}$$

$$\epsilon_t^\pi \sim N(0, e^{h_t})$$

$$h_t = h_{t-1} + \epsilon_t^h$$

$$\epsilon_t^h \sim N(0, \sigma_h^2)$$

$$\epsilon^{\rho^\pi} \sim TN(-\rho_{t-1}^\pi, 1 - \rho_{t-1}^\pi; 0, \sigma_{\rho^\pi}^2)$$

ag. PC

$$\pi_t - \tau_t^\pi = \rho_t^\pi(\pi_{t-1} - \tau_{t-1}^{\pi,EU}) + \lambda_t(u_t - \tau_t^u) + \beta_t \pi^{oil} + \epsilon_t^\pi$$

$$(u_t - \tau_t^u) = \rho_1^u(u_{t-1} - \tau_{t-1}^u) + \rho_{n,2}^u(u_{t-2} - \tau_{t-2}^u) + \epsilon_t^u$$

$$\tau_t^{\pi,EU} = \tau_{t-1}^{\pi,EU} + \epsilon_t^{\tau,\pi}$$

$$\tau_t^u = \tau_{t-1}^u + \epsilon_t^{\tau,u} \quad \epsilon_t^h \sim N(0, \sigma_h^2)$$

$$\rho_t^\pi = \rho_{t-1}^\pi + \epsilon_t^{\rho,\pi} \quad \epsilon_t^u \sim N(0, \sigma_u^2)$$

$$\lambda_t = \lambda_{t-1} + \epsilon_t^\lambda \quad \epsilon^{\rho^\pi} \sim TN(-\rho_{t-1}^\pi, 1 - \rho_{t-1}^\pi; 0, \sigma_{\rho^\pi}^2)$$

$$\epsilon_{n,t}^\pi \sim N(0, e^{h_t}) \quad \epsilon^\lambda \sim TN(-1 - \lambda_{t-1}, 0 - \lambda_{t-1}; 0, \sigma_\lambda^2)$$

$$h_t = h_{t-1} + \epsilon_t^h \quad \epsilon^\beta \sim TN(-\beta_{t-1}, 1 - \beta_{t-1}; 0, \sigma_\beta^2)$$

7.4 Prior predictive analysis

To emphasize the sensibility of our prior settings we perform a prior predictive analysis. Therefore, we draw from the prior distribution using the starting values and priors shown in table 2 and simulate with the state equations as to generate artificial data series for inflation and unemployment. We repeat this exercise 10^4 times, whereby we compute the mean, the median, the 16%- and 84%-percentile as well as the variance of each draw of the artificial series. We can then evaluate the observed data with the cumulative density functions from the artificial data series. Table 3 presents the prior cdfs evaluate at the observed data for the distinct features. It can be seen that the baseline model explains well the observed data.

Table 3: Prior cdfs for observed data of inflation and unemployment

	inflation	unemployment
mean	0.50	0.68
median	0.49	0.40
16%	0.50	0.31
84%	0.50	0.94
variance	0.50	0.89

7.5 Forecasting results on EMU unemployment rates

Turning to the evaluation of unemployment forecasts, aggregate Phillips curves and the UC models offer a substantial improvement in forecasting, compared to the AR and RW models. Panel model variants, however, again perform best from horizon 12 onwards. This implies that variations of the panel PC model only change the forecasting performance marginally across models (ratios show some variations from the third decimal point onwards). Using cumulated oil price inflation improves the unemployment forecast for the medium term. Thus, our proposed panel Phillips curve specification reveals a better forecast accuracy of EU10 inflation and unemployment (from the medium term onwards) than a variety of other UCSV and univariate time-series models.

Table 4: EU10 unemployment: RMSFEs relative to RMSFE of the ARIMA(1,0,1) model

model	horizon													
	1	2	4	6	9	12	15	18	21	24	27	30	33	36
ARIMA(1,0,1)	1	1	1	1	1	1	1	1	1	1	1	1	1	1
ARIMA(2,0,1)	1.04	0.96	0.70	0.73	0.87	0.98	1.08	1.14	1.18	1.18	1.16	1.12	1.09	1.07
ARIMA(2,0,2)	0.98	0.87	0.76	0.77	0.87	0.95	1.01	1.07	1.09	1.10	1.10	1.07	1.05	1.03
ARIMA(1,0,2)	1.00	0.89	0.91	0.91	0.94	0.96	0.97	0.98	0.99	0.99	0.99	0.99	0.99	0.99
RW	1.01	1.01	1.03	1.02	1.02	1.01	1.01	1.00	1.00	1.00	1.00	1.00	1.00	1.00
panel PC	0.31	0.49	0.74	0.84	0.90	0.92	0.94	0.95	0.94	0.94	0.95	0.95	0.94	0.95
panel PC excl. oil	0.31	0.49	0.74	0.83	0.90	0.92	0.93	0.94	0.93	0.94	0.94	0.94	0.94	0.94
ag. PC	0.65	0.88	1.16	1.31	1.38	1.37	1.34	1.28	1.24	1.21	1.19	1.17	1.15	1.15
ag. PC excl. oil	0.41	0.73	1.19	1.41	1.52	1.51	1.47	1.41	1.35	1.30	1.27	1.24	1.21	1.20
UC	0.52	0.66	1.00	1.28	1.51	1.59	1.61	1.56	1.51	1.47	1.43	1.40	1.37	1.36
panel PC const. λ	0.31	0.49	0.73	0.83	0.90	0.92	0.94	0.95	0.94	0.95	0.95	0.95	0.94	0.95
panel PC const. ρ	0.31	0.50	0.75	0.85	0.92	0.94	0.95	0.96	0.95	0.96	0.96	0.96	0.95	0.96
panel PC const. σ	0.31	0.49	0.74	0.83	0.90	0.92	0.93	0.94	0.94	0.94	0.95	0.95	0.94	0.95
panel PC const. ω	0.31	0.50	0.75	0.85	0.92	0.95	0.96	0.96	0.95	0.95	0.96	0.95	0.95	0.95
panel PC excl. sv	0.30	0.49	0.73	0.83	0.90	0.93	0.94	0.95	0.95	0.96	0.96	0.96	0.96	0.96
panel PC cum. oil	0.30	0.49	0.73	0.83	0.89	0.91	0.93	0.94	0.93	0.94	0.94	0.94	0.94	0.94
panel PC cs ρ	0.31	0.50	0.74	0.84	0.91	0.93	0.94	0.95	0.95	0.95	0.96	0.96	0.96	0.96

This table displays the root mean squared forecast errors (RMSFE) of respective model relative to the RMSFE of an AR(2) model that stem from a pseudo-out-of-sample unemployment rate forecast for the time span January 2009 to April 2017. Values lower than 1 indicate that the RMSFE of the respective model is lower than those of the AR(1) model. The results from the benchmark model are highlighted in bold. The shading indicates the respective forecasting performance, whereby green (light) shadings emphasize better forecasting performance.

Halle Institute for Economic Research –
Member of the Leibniz Association

Kleine Maerkerstrasse 8
D-06108 Halle (Saale), Germany

Postal Adress: P.O. Box 11 03 61
D-06017 Halle (Saale), Germany

Tel +49 345 7753 60
Fax +49 345 7753 820

www.iwh-halle.de

ISSN 2194-2188